*energies*

MDPI

*Review*

# Performance Prediction of Plate-Finned Tube Heat Exchangers for Refrigeration: A Review on Modeling and Optimization Methods

**Silvia Macchitella [1], Gianpiero Colangelo [1] and Giuseppe Starace [2,*]**

[1] Department of Engineering of Innovation, University of Salento, Via per Monteroni, 73100 Lecce, Italy
[2] Dipartimento di Management, Finanza e Tecnologia, Università LUM, SS100 km 18, 70010 Casamassima, Italy
* Correspondence: starace@lum.it

**Abstract:** Finned tube heat exchangers are used in many technological applications in both civil and industrial sectors. Their large-scale use requires a design aimed at reaching high thermal efficiency as well as avoiding unnecessary waste of resources in terms of time and costs. Therefore, in the last decades, research in this area has developed considerably and numerous studies have been conducted on modeling in order to predict heat exchangers (HXs) performance and to optimize design parameters. In this paper, the main studies carried out on plate-finned tube HXs have been collected, analyzed, and summarized, classifying existing models by their scale approach (small, large, or multi-scale). In addition, the main methods of design optimization with a focus on circuitry configurations have been illustrated. Finally, future developments and research areas that need more in-depth analysis have been identified and discussed.

**Keywords:** heat exchanger; design; model; optimization; hybrid method; evaporator; performance; multi-scale model; circuit arrangement; refrigerant circuit layout



**Citation:** Macchitella, S.; Colangelo, G.; Starace, G. Performance Prediction of Plate-Finned Tube Heat Exchangers for Refrigeration: A Review on Modeling and Optimization Methods. *Energies* **2023**, *16*, 1948. https://doi.org/10.3390/en16041948

Academic Editors: Pavel Skripov and Aleksandr Pavlenko

Received: 13 December 2022
Revised: 31 January 2023
Accepted: 13 February 2023
Published: 15 February 2023



## 1. Introduction

Heat exchangers (HXs) are devices that provide heat transmission between two or more fluids at different temperatures [1]. It is of great importance to ensure optimum performance as they are employed in a wide range of engineering applications, such as process, power production, food and chemical applications, manufacturing industry, refrigeration, air-conditioning, electronics, and space applications. Since they are so widespread, there are different types of HXs as well as different classifications have been proposed based on the construction, heat transfer process, surface compactness, flow arrangement, heat transfer mechanism, and number of fluids [2]. Figure 1 shows the most common classification according to construction.

A finned tube HX is made up of a number of tubes with fins attached to the outside which can be normal, transverse, helical, or longitudinal to the tube. Similarly, continuous plate-fin sheets may be attached to the array of tubes by a tight mechanical (press) fit, adhesive bonding, tension winding, soldering, brazing, welding, or extrusion, which can be organized in a staggered or in-line form.

In this type of coil, a fluid for heat transmission, such as oil, water, or refrigerant, flows inside round, rectangular, or elliptical-shaped tubes exchanging heat with another medium, such as air, which flows between the fins. A good overview of the thermal characteristics of plate-finned and unfinned tube heat exchangers can be found in [3] where the authors address not only the most important thermofluid correlations, but also the influence of the most important design parameters on the performance of HXs. The impact of the fin type and geometry on the performance is instead discussed extensively by Basavarajappa [4] who concluded that better performance can be obtained with a larger fin area and by creating turbulence in the fluid, which also causes bulk fluid mixing.

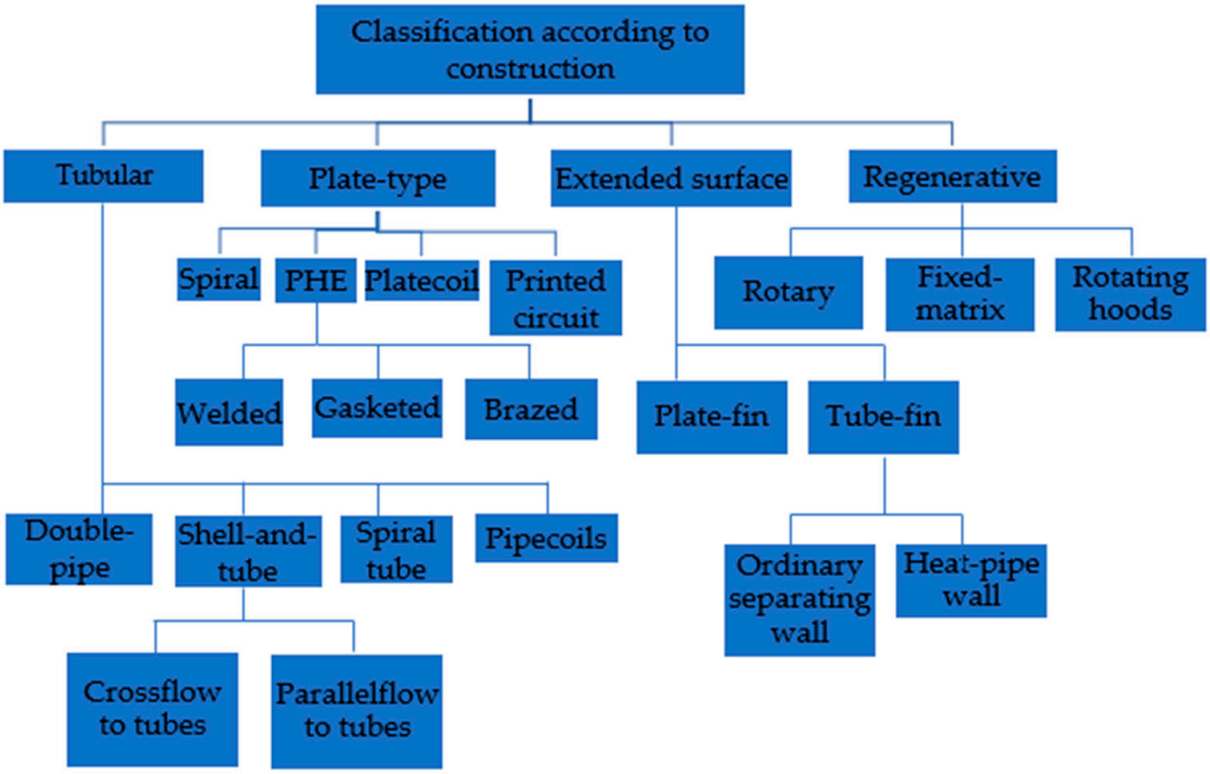


**Figure 1.** Classification of HXs based on construction.

Some of the extended surface exchangers are compact: an HX with a surface area density greater than 700 $m^2/m^3$ is defined as a compact heat exchanger (CHX), when it is above 10.000 $m^2/m^3$ it can be classified as a micro heat exchanger [5]. CHXs of plate-fin and tube-fin types are widely used as vehicular HXs, evaporators and condensers in refrigeration, in the air-conditioning industry, automotive radiators, etc. Their strengths can be compactness as well as lightness and reduced production costs simultaneously achieving high heat transfer performance with low pressure drop. Compact heat exchangers' most recent scientific and technological advances are illustrated in [6–8]. Following a life-cycle approach, Hesselgreaves et al. [6] shared an interesting exergetic analysis of heat exchangers seen as part of a system. The same method was applied by Zohuri [7], who performed a thermal study beginning with the design of compact heat exchangers and continuing through the operational and safety steps. In his work, Zohuri also suggested alternative designs with the aim to maximize the exchanger heat transfer rate. The reduction of fouling in heat exchangers and their systems, however, is given special attention by Klemes et al. [8], who describe fouling deposition and threshold fouling mechanisms and also offer practical knowledge of the most recent process integration techniques.

Furthermore, different fin configurations are possible for finned tube heat exchangers, as shown in Figure 2. It has been shown that the fin type and geometry are some of the parameters that most influence the performance of an exchanger both in terms of heat transfer rate and pressure drops [9]. The HXs with fins that generate turbulent flow through corrugation, louvers, and vortex generators develop a greater heat transfer rate, but, on the other hand, there is an increase in flow resistance and therefore an increase in pressure drops.

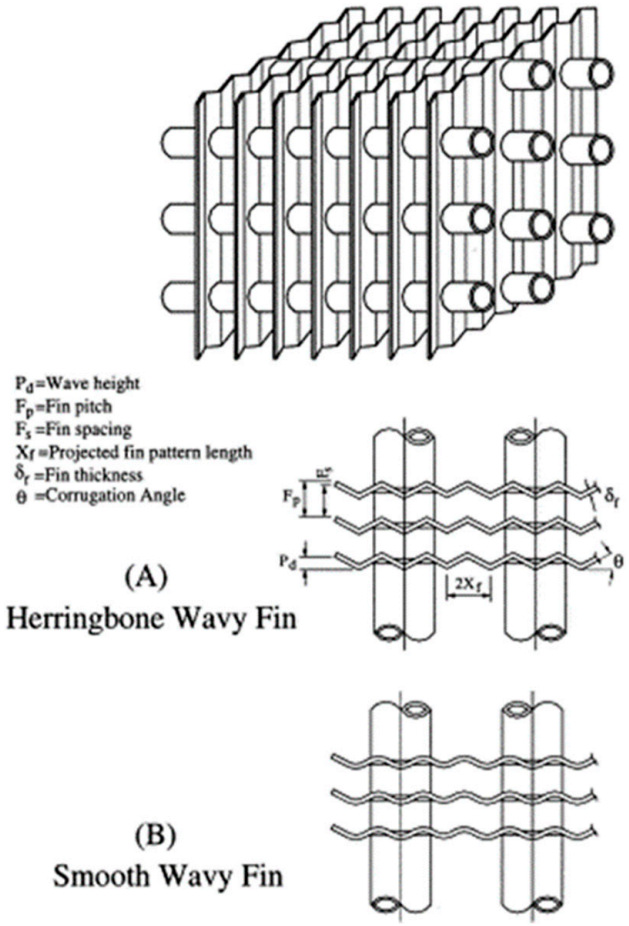


**Figure 2.** Different fin types for wavy finned tube heat exchangers [9].

In the last decades, the growing cost of energy and raw materials has forced more and more efficient design of heat exchangers to avoid unnecessary oversizing or malfunctions of these devices. So various mathematical models, and analytical and experimental studies were developed to model the HXs and predict, as efficiently as possible, the performances in terms of heat transfer rate and pressure drops. In this review paper, the main models for predicting the performance of plate-finned tube exchangers will be discussed and analyzed in detail, classifying them by their approach scale as small, large, or multi-scale models. Moreover, many efforts have been made by researchers to identify the optimal configuration of an exchanger as well as many useful tools to optimize their performance according to operating conditions. Therefore, in the second part of this work the main optimization techniques will be illustrated together with the geometric parameters that most influence HXs performance. Finally, the most promising future research paths will be analyzed to identify research areas that would be better to deepen with future research.

## 2. Heat Exchanger Design Procedure

The design process of a heat exchanger is a very complex problem as there are many involved parameters to take into account, with complex correlations. Establishing a correct design procedure is the first step for designing an efficient exchanger and avoiding malfunctions. The design aim is certainly to satisfy the process requirements; therefore the designers must obtain all the information such as fluids flow rates, operating and maximum pressures, temperatures, and also all the constraints of cost, space, and types of materials. A schematic representation of a typical design procedure can be seen in Figure 3. Designers select the construction type of the device, geometry, and all the materials involved, tak-

ing into consideration not only the operating conditions but also issues concerning costs, maintenance, reliability, and safety of the device.

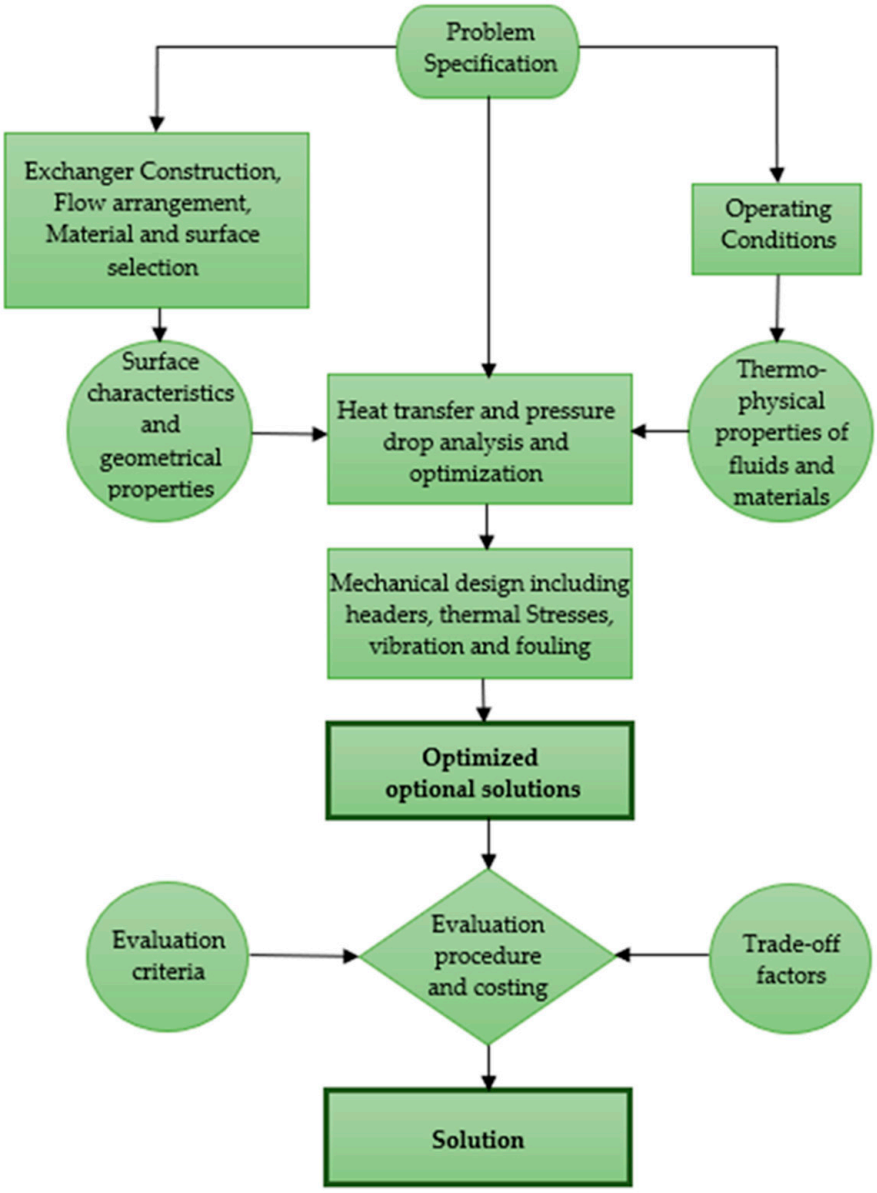


**Figure 3.** Schematic representation of heat exchanger design methodology.

The HX design process can be classified as a sizing problem (design problem), where the goal is to determine the size of the exchanger, or a rating (performance analysis), where the exchanger already exists or has been chosen and the performance needs to be assessed [10]. Often, the solutions to this problem are many and then the choice is guided by other criteria such as costs. If the chosen exchanger does not fully satisfy all the requirements, another design must be chosen through an iterative procedure. Once the thermohydraulic performance design has been completed, the second step is to determine the mechanical properties by the design of inlet and outlet nozzles, connectors, temperature and pressure measurement devices, etc. In addition, steady-state and transient thermal stress studies must also be performed. Another very important aspect is maintenance: the positioning and configuration of the exchanger must allow correct cleaning and easy accessibility to all the components, especially those most exposed to problems of corrosion, erosion, and vibrations. Once the mechanical design has also been completed, the cost

analysis has to be performed to obtain to the optimal solution of an exchanger that satisfies all the requirements at the minimum cost. The costs of materials, manufacturing, testing, installation, operation, and maintenance have to be included in the analysis.

## 3. Heat Exchanger Modelling Methods

An act to quantitatively characterize a natural phenomenon is known as a mathematical model [11]. There are many different ways that mathematical models can be expressed. For example, they can be deterministic or stochastic, some can treat time as a discrete entity while others do not, and some models seek to provide analytical correlations between variables while others define how those variables change over time. Another classification is possible by their scale approach: small, large, or multi-scale models (Figure 4). Typically, small-scale models are numerical models built with the help of CFD techniques, i.e., a set of techniques that, through the aid of computational systems, allow simulation of the dynamics of fluids. Often these models are very accurate in their results as they study the phenomena in detail of small-scale interactions. On the other hand, however, they are often expensive in terms of time and therefore costs and, in most cases, they do not match with the requests of the manufacturing companies that must respond more and more promptly to market demands. On the contrary, large-scale approach models are simpler and faster to apply and are very useful for manufacturing companies. Typically, these are analytical models that often come from experimental tests. The disadvantage of these models lies in the fact that the results can be slightly inaccurate. As a consequence, devices designed with purely analytical models could be oversized and, therefore, result in a waste of money or even undersized giving rise to malfunctions. Moreover, often a wrong design cannot be detected before production and installation, generating an unnecessary and harmful waste of resources.

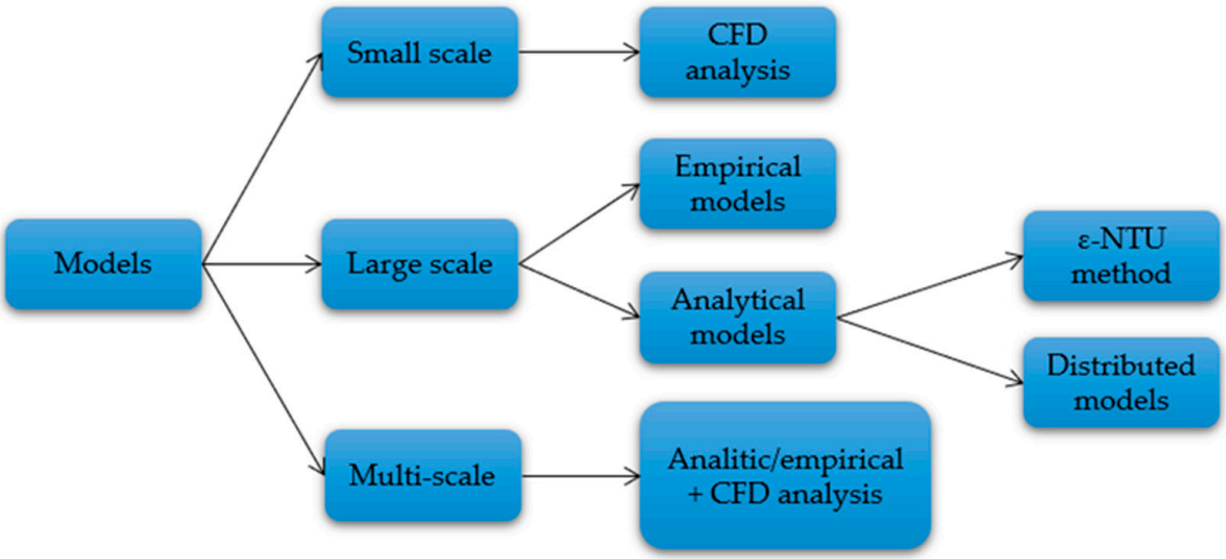


**Figure 4.** Classification for HX modelling.

Still, in the category of large-scale models, those that come from pure experimental tests are included. These are accurate in most cases but have the disadvantage of being highly dependent on the device's geometry, operating at boundary conditions of the specific test. In other words, experimental tests often provide slightly flexible results, and therefore are not adaptable to other working conditions.

Another category of models that combines the accuracy advantages of small-scale models and the relative simplicity and speed of application of large-scale models are the so-called "multi-scale" models.

Therefore, each design method has advantages and disadvantages (see Table 1) and currently the choice of the model to use by manufacturing companies is often guided by time and cost issues, as well as the specific application of the device.

**Table 1.** Summary of design methods with the indication of advantages and disadvantages.

| Models | Advantages | Disadvantages |
| --- | --- | --- |
| CFD models | Very accurate results | Expensive in terms of time and costs |
| Empirical models | Accurate results | Results highly depending on specific geometry and boundary conditions |
| Analytical models | Relatively easy and quick to apply | Poor accuracy of the results |
| Multi-scale models | Relatively easy and quick to apply<br>Very accurate/accurate results (*) | Not simple model development. Further research is needed in the future |

(*) Accuracy depends on the model used.

In this section, a complete overview of the methods for the modelling of plate-finned tube heat exchangers is illustrated, resulting in a classification based on their scale approach together with an introduction of the main experimental correlations developed by researchers for the calculation of the thermodynamic properties of the fluids.

### *3.1. Large Scale Models: Experimental Correlations for Fluid Properties Calculation*

Over the past few decades there have been several experimental studies concerning the heat transfer properties of plate-finned tube exchangers carried out by researchers. As a result, many correlations regarding the characteristics of the fluids and the pressure drops were developed and then used in different ways.

Colburn, who performed his first research studies in heat transfer in 1930, proposed a method for the correlation of forced convection heat-transfer data coming from experimental tests, by plotting a dimensionless group—which represents this dataset—against the Reynolds number [12]. The method is particularly appreciable in the transition region between laminar and turbulent flow inside the tubes, where the heat transfer factors can show inflections. Rosman et al. [13] performed several tests to measure the overall heat transfer coefficients for two-row tube and plate-fin exchangers. Results were combined with measurements from the literature on one-row exchangers to shift from the local mass transfer coefficient to the local heat transfer coefficient. Moreover, the same authors carried out a numerical analysis to obtain the temperature distribution and fin efficiency. Dittus and Boelter [14] conducted a substantial and systematic work measuring the film transfer factors on the liquid side of a radiator, dividing the results by turbulent, viscous, and non-turbulent flow and by the number of rows in the exchanger. Another type of tube shape was studied by Merker [15], who carried out measurements of heat transfer and pressure drop on elliptical tube banks with a staggered arrangement and different transversal and longitudinal pitches. The results showed that exchangers with elliptical-shaped tubes have a smaller front area on the shell side compared to those with a circular one. Wang et al. [16] proposed a modification of the well-known Žukauskas correlation [17]—which worked for multiple-row heat exchangers—extending its applicability for 1-row HX and $Re < 1000$. Tests were performed on tube banks with a different row number (from one to six) and results confirmed that heat transfer coefficients increase with the row number, while they are comparable for 1-row and 2-row tube banks. Moreover, for 2-row HX the heat transfer coefficients were found to be higher with smaller tube diameters, at the same transversal pitch, while they are comparable for 1-row HX. Kim and Kim [18] experimentally investigated HXs with large fin pitches by varying fin pitch, the number of tube rows, and tube arrangement. Fin pitch was found to have less influence on the heat transfer coefficient for 1-row exchangers with larger fin pitch, but it had more influence on multiple-row coils

since the heat transfer coefficient increased as the fin pitch became higher. Moreover, results showed that the heat transfer coefficient decreased as the number of tube rows increased in all cases apart from the staggered arrangement with 4-rows, where the influence of row number was found to be quite negligible. However, a staggered tube configuration showed a heat transfer coefficient 10% higher compared to the in-line arrangement. Furthermore, Khan et al. [19] carried out experimental tests on an array of 18 elliptical tubes both on air cooling and heating using water as a working fluid. The heat transfer coefficient was found to be higher in cooling than in the heating process and the results showed good accordance with the developed correlation. A good adherence between numerical study and experimental tests was reached by Paeng et al. [20] who investigated the air-side forced convective heat transfer of a geometrically defined staggered heat exchanger. Results showed a discordance of less than 6% of the average Nusselt numbers between numerical and experimental data, with Reynolds number between 1082 and 1649. In his work, Taler [21] presented an experimental–numerical method for determining heat transfer correlations for both fluids involved in cross-flow exchangers with extended surfaces. The method is based on a non-linear regression technique that allows calculating of the coefficients in the Nusselt number correlations by using high-quality experimental data.

Figure 5 shows a schematic representation of a typical experimental setup for tests on HXs.

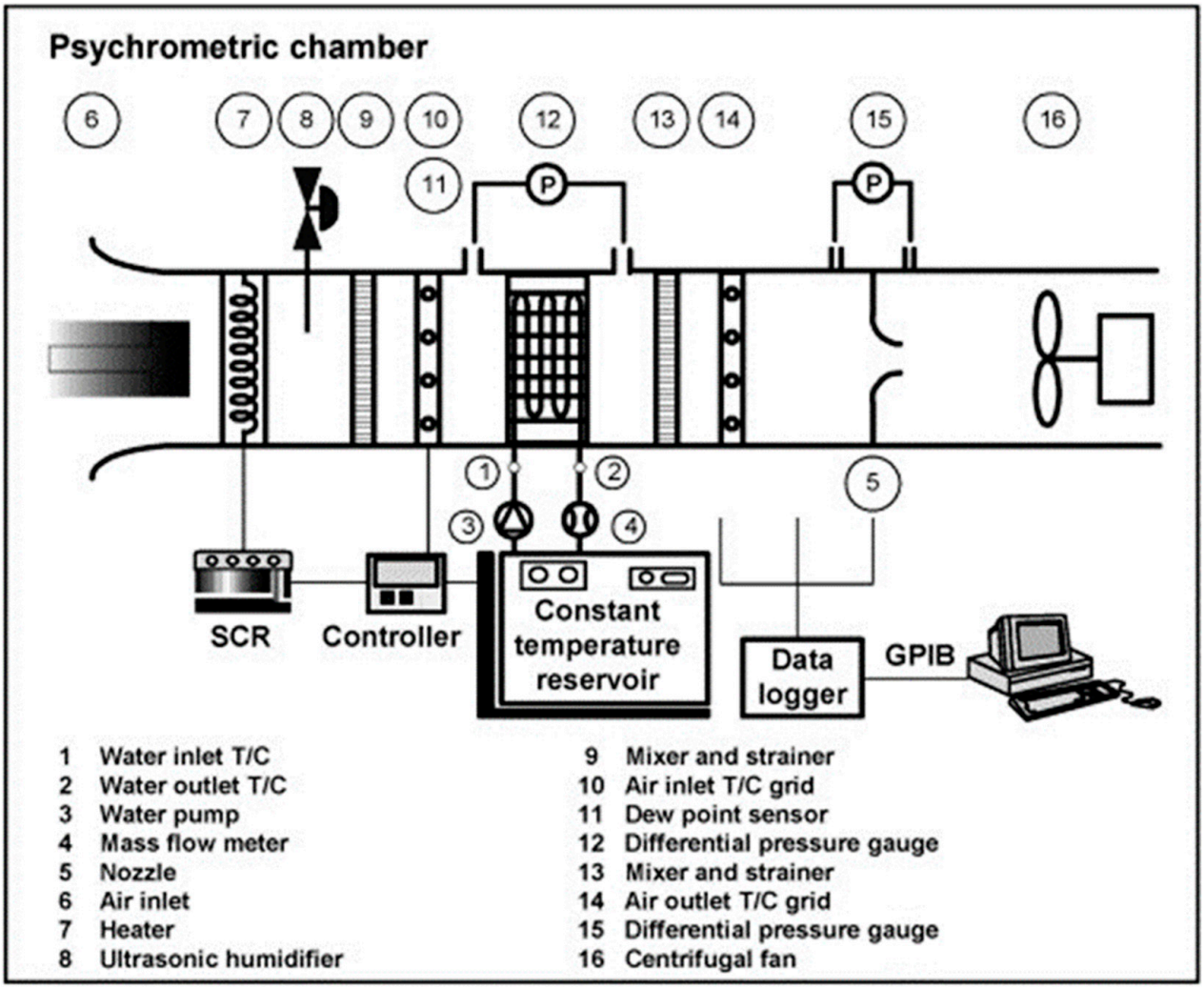


**Figure 5.** Schematic representation of a typical experimental setup [18].

Recent experimental studies focused on analyzing the influence of several geometric features on the HX overall performance. Some important factors impacting a finned and tube HX performance, including fin type (louvered and wavy), fin pitch, and the row number, were experimentally evaluated by Okbaz et al. [22] in their work. Results show that Colburn-j factor values of the louvered fin configuration are higher than those of the wavy fin for all the considered cases at all Reynolds numbers. On the other hand, the pressure drop associated with louvered fin HXs was higher if compared to wavy fin HX. The number of tube rows and fin pitch were also investigated by Bozkula and Demir [23], together with frontal air velocity, temperature, and relative humidity of nine different exchangers under dry and wet conditions. Moreover, three different types of correlations (multivariate first-order polynomial equations) are provided for the $j$ factor and $f$ factor under dry and wet conditions, showing a good agreement with the experimental data. Fin characteristics were found to have a great influence on HXs, especially under frosting conditions, by Wu et al. [24]. Experimental tests were performed to compare the performance of two evaporators with different fin features (corrugated and plain fins), under different outdoor conditions such as air temperature, relative humidity, and wind speed. Plain fin HX results in higher thermal performance compared to corrugated fin HX under frosting conditions.

Tube arrangement (staggered vs. in-line) was investigated by Che and Elbel [25], who carried out tests using a coating material with color change properties and a tracer gas to measure the local mass transfer on the fin surfaces of two staggered/in-line tube HXs. Then, local air-side heat transfer coefficients (HTCs) were calculated. Comparison between the average HTCs for each row of the two exchangers suggests that the staggered configuration suffers less deterioration of HTC than the HX with in-line tube arrangement. Moreover, HTC decreasing through the rows is also influenced by the air velocity and the row number.

The coefficient of performance (COP) and the dimensionless heat transfer volumetric density $\widetilde{q}$ were used by Matos et al. [26] to experimentally compare the performance of two split air conditioning systems, having evaporators with circular and elliptic tube shapes. The conditioning unit with elliptic tube evaporators showed better performance than the one with a circular tube shape.

Very interesting experimental studies were recently conducted by Sim et al. [27] and Wang et al. [28] on finned-tube heat exchangers with reversely-variable circuitry to improve performance. The conventional FTHXs have two-way fixed circuitry with the same refrigerant flow path in the opposite direction both when the heat pump is used in the heating and cooling process. Tests performed by Wang et al. [28] demonstrated that the overall energy performance of a heat pump improved by giving a certain circuitry arrangement flexibility to the exchanger when it worked as an evaporator or condenser.

In Table 2, some of the well-known correlations have been selected concerning their application ranges and cataloged by subdividing them according to HX tube arrangement and tube shape. The correlations are obtained through experimental investigations on finned tubes, unfinned tubes, or tube banks, therefore they cannot be compared with each other. The purpose of the table is to show that the correlations are strongly dependent not only on the boundary conditions, but also on the specific geometric configuration of the tested device and, therefore, it cannot be considered exhaustive.

**Table 2.** Selected experimental correlations for plate-finned tube exchangers.

| No. | Tube Arrangement | | Tube Shape | | Experimental Correlation | Range of Application | Ref. |
|---|---|---|---|---|---|---|---|
| | Staggered | In-Lined | Circular | Elliptical | | | |
| 1 | - | - | - | - | $Nu = 0.33 \times Re^{0.6} Pr^{1/3}$ | $10 \ll Re \ll 4 \times 10^4$ | [12] |
| 2 | | x | x | | $\overline{Nu} = \left[3.58 + 8.46 \times 10^{-4} Re^{1.24}\right] \times Pr^{0.4}$ | $200 \ll Re \ll 1700$ | [13] |
| 3 | | x | - | - | $Nu = 0.023 \times Re^{0.8} Pr^{0.3}$ | $Re \geq 1 \times 10^4$<br>$0.7 \leq Pr \leq 100$<br>$L/D \geq 60$ | [14] |
| 4 | x | | | x | $Sh = 1.181 \times Re^{0.480}$<br>$Sh = 1.212 \times Re^{0.676}$ | $P_L = 1.0$<br>$1.97 \leq P_T \leq 3.16$ | [15] |
| 5 | | x | x | | $Nu = 1.7 \times Nu_z$ (*)<br>$Nu = 1.38 \times Nu_z$ (*) | $N_R > 1$; $Re < 500$;<br>$N_R > 1$; $500 < Re < 1000$ | [16] |
| 6 | x | | x | | $j = 0.710 \times Re_{Dh} \times N_R - 0.141 p_F 0.384$ | $600 \ll Re_{Dh} \ll 2000$<br>$7.5 \ll p_F \ll 15$<br>$1 \ll N_R \ll 4$ | [18] |
| 7 | | x | | x | $Nu = 0.33 \times Re^{0.64} Pr^{1/3}$ | $1 \times 10^4 \ll Re \ll 3.6 \times 10^4$ | [19] |
| 8 | x | | x | | $Nu = 0.049 \times (Re_D)^{0.784} \left(Pr_f\right)^{1/3}$ | $1082 \ll Re_D \ll 1649$ | [20] |
| 9 | x | | | x | $Nu = 0.085 \times Re^{0.712} Pr^{1/3}$ | $150 \leq Re \leq 350$ | [21] |

(*) where $Nu_z = FCRe_D^m Pr^n \left(\frac{Pr}{Pr_w}\right)^{0.25}$ where $F$ is a correction factor for the number of tube rows, and $C$, $m$, $n$ depending on $Re_D$. $Pr_w$ valuated at wall temperature $T_w$.

### *3.2. Large Scale Models: Analytical and Semi-Analytical Studies*

The modeling of tube and fin heat exchangers can be challenging due to their complex geometry. In addition, when the HX works as an evaporator or condenser, due to the presence of a two-phase flow, condensate mass transfer, and a heat transfer involving humid air flow, it may be more and more difficult. In the last few years, considerable efforts have been directed to develop analytical and semi-analytical models that can be roughly classified into ε-NTU models and distributed models (tube-by-tube or control volume approach models).

In 1955, Kays and London [29] developed the ε-NTU method with the aim to simplify heat exchanger analysis by introducing the heat transfer effectiveness, ε, calculated as the ratio of the actual heat transferred to the greatest amount of heat that may possibly be transferred in an indefinitely long heat exchanger. The ε-NTU method was improved by Browne and Bansal [30] using an elementary strategy. Their model makes it possible to account for the various heat transfer coefficients present throughout the HXs, enhancing the model's physical realism and accuracy. However, in practice, the ε-NTU's applicability is severely constrained because an isothermal condition can exist only when the capacity ratio is equal to zero [31].

In the distributed models, the HX is divided into multiple segments or control volumes (cells) where one control volume's outlet serves as the intake to another neighboring cell. Compared with the ε-NTU models, the distributed models provide more accuracy in the dynamic behavior of the exchanger.

A control volume approach was used by Corberán et al. [32,33] who developed a distributed model for finned exchangers working as evaporators and condensers which involves an iterative calculation to obtain the pressure and temperature characteristics both on the air and the refrigerant side and including mass, energy, and momentum equations.

A general-purpose simulation and design tool (called CoilDesigner) using a "segment-by-segment" technique for air-to-refrigerant heat exchangers was developed by Jiang et al. [34]. The model can be applied to a generic finned tube coil (Figure 6) with an arbitrary refrigerant circuitry layout, numerous working fluids, and no limitations on the quantity and placement of the intake and outlet streams. The intersection where two tubes are connected together is referred to as a junction, and a junction-tube connectivity matrix is generated to represent the relationship between junctions and tubes (Figure 7). Each finned

tube is divided into $N_{seg}$ segments to account for non-uniform air distribution, heterogeneous characteristics, and heat transfer coefficients of the refrigerant (Figure 8). According to the order in which the refrigerant flows through the tube, the segments are numbered from 1 to $N_{seg}$. The authors validated the model by comparing the simulation results data coming from experimental investigations carried out by McQuiston [35], showing an overall agreement of 10%.

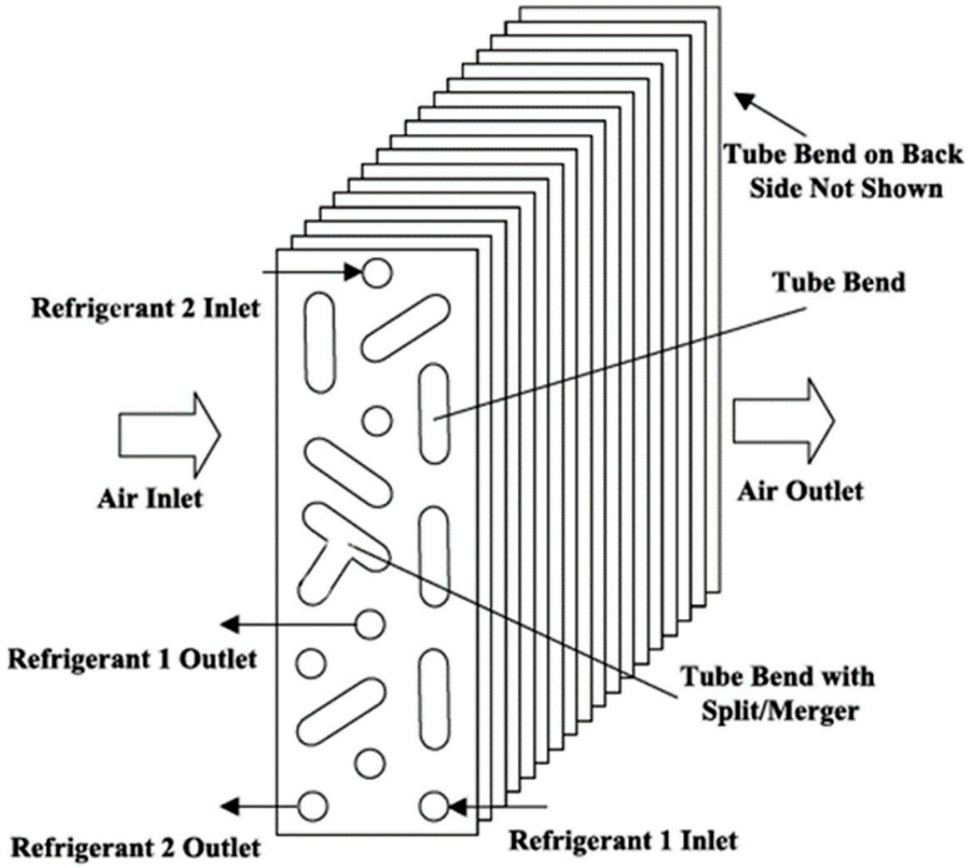


**Figure 6.** Representation of a finned tube coil for modeling [34].

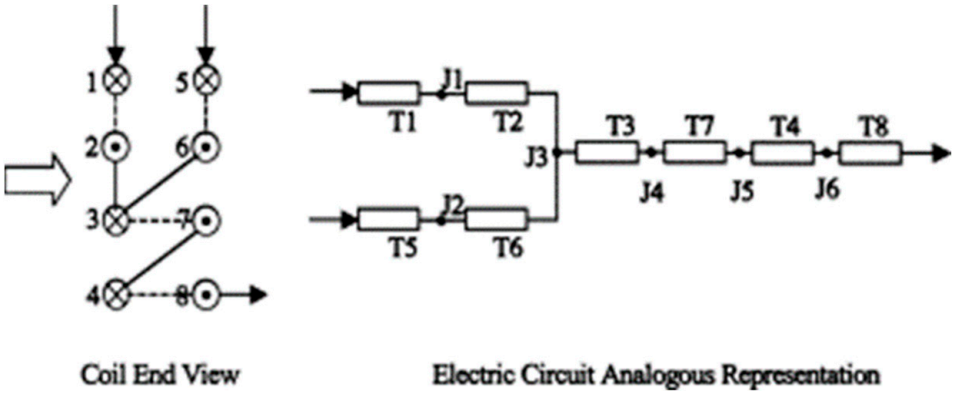


**Figure 7.** Electric network-like representation of tube connections [34]. Rectangles represents tubes, each dot is a junction.

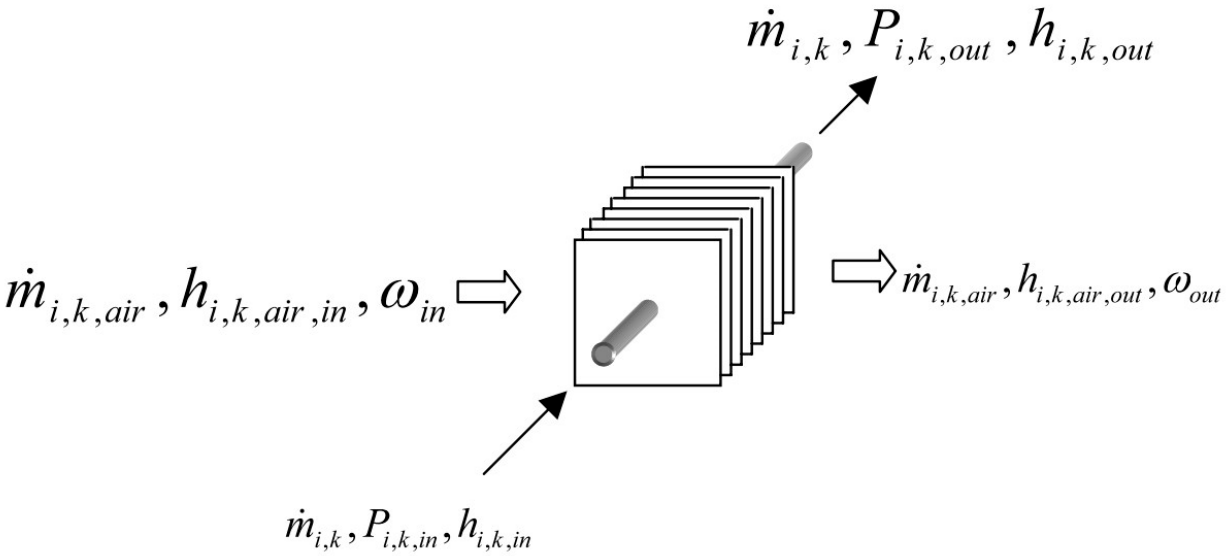


**Figure 8.** Segment as a single cross-flow heat exchanger [34].

A mathematical model using the segment-by-segment approach was implemented by Tarrad and Al-Nadawi [36] with the aim to predict the performance of a louvered finned tube evaporator working with pure and zeotropic refrigerants. A good match between numerical results and data coming from experimental tests conducted on an air-conditioner unit was shown.

Joppolo et al. [37] studied the influence of circuitry layout on the performance of a plate-finned tube condenser by developing a numerical model based on the finite volume approach by dividing each tube into volume cells and solving the equations iteratively by following the flow path.

Another model based on a control volume approach suitable for finned tube evaporators in order to study the flow characteristics inside the tubes was implemented by Tong et al. [38]. Results showed that the fluid follows an annular pattern. Moreover, an experimental investigation was carried out obtaining good agreement with simulated data.

Domanski [39,40] proposed the EVAP-COND tool, which is based on the tube-by-tube method and has a visual interface. This model enables the handling of complex refrigerant circuitry layouts, modeling the fluid distribution between circuits, and accounting for non-uniform air distribution. By combining the simulated performance of each tube, the evaporator's capacity is determined. Local parameters for each tube can then be obtained, such as inlet and outlet temperatures for air and temperature, pressure drop, mass flow rate, enthalpy, and inlet and outlet quality for the refrigerant. Model validation results provided good confidence for the performance prediction.

A flexible model, based on the discretization technique for the calculation of finned HX performance, was developed by Bensafi et al. [41]. Water, R134a, R22, and refrigerant combinations based on R125, R32, and R134a can all be used in single-phase HX, evaporators and condensers. In addition, the model can manage different circuitry layouts, non-uniform air distribution, plain, wavy, and louvered fins, and smooth and internally finned tubes. Validation tests showed good accordance with experimental data of less than 5% for the heat capacity. On the other hand, a high deviation of about 30% between simulation and experimental data was found for pressure drops.

Furthermore, Liang et al.'s [42] distributed simulation model uses a control volume approach with chosen governing equations to predict the performance of evaporators with complex circuitry layouts. Utilizing refrigerant R134a, the model is validated by matching experimental data with simulated values. Under various airflow conditions, the simulated cooling loads produce results that are 5% different from the measured values.

The refrigerant pressure drops calculated through the simulation model are within 25% of the measured values.

An effort to give a better match with real performance was made by Ding et al. [43] who developed an evaporator model combining the advantages of empirical and analytical models. Process fundamental governing equations are formulated together with selecting the input/output variables responsible for the system performance, which can be measured and controlled. Variables that cannot be measured are represented as simple functions of selected input/outputs or constraints, obtaining a single equation that can correlate system input and outputs. Unknown parameters are identified by linear or nonlinear least-squares methods. In order to validate the model, heat transfer rate simulated data were compared with data coming from experimental tests and a deviation of 8% was found.

A model for simulating air-to-refrigerant heat exchangers that takes into consideration conduction through the fins was proposed by Singh et al. [44]. This model was created as a versatile and all-purpose simulation tool and is based on a segment-by-segment methodology. The heat exchanger is spatially simulated on a Cartesian grid to account for fin conduction, resulting in temperature distribution over the fin surface (Figure 9). The model's prediction results are checked against experimental data collected from literature and experimental tests. Predicted temperatures on tube-bends agree within 3.9 °C and overall heat load agrees within a maximum of 5% with respect to measured data.

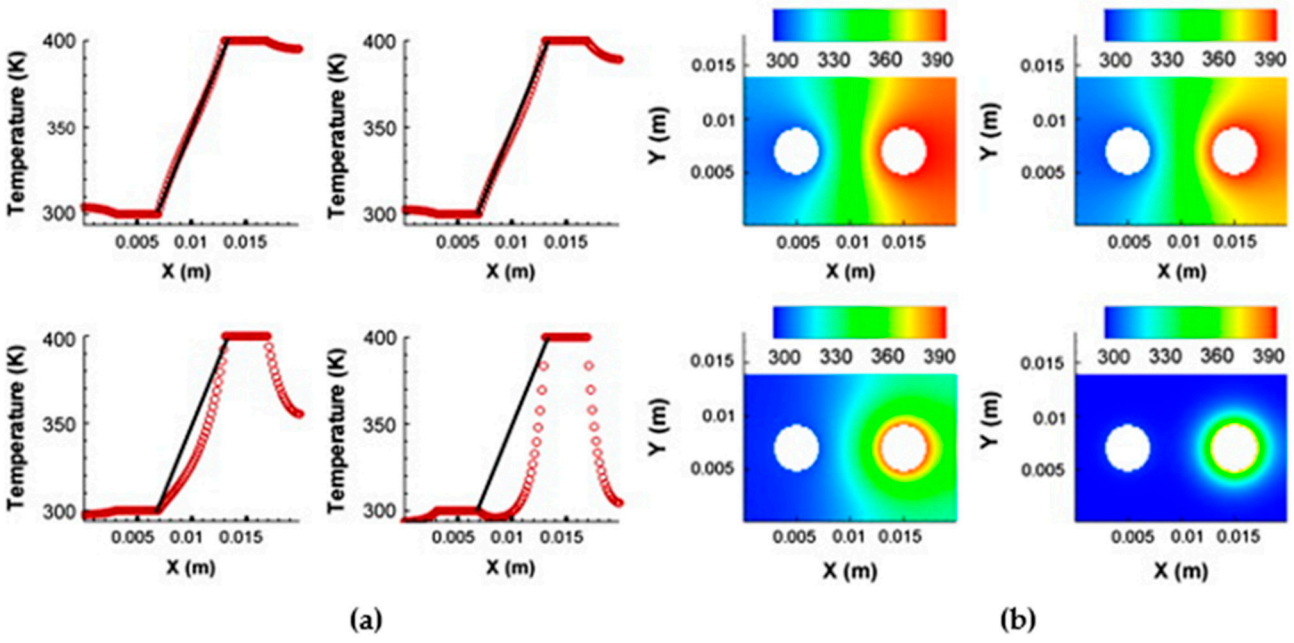


**Figure 9.** Temperature distribution along the longitudinal section of the fin (**a**) and over the whole surface (**b**) for increasing air heat transfer coefficient from 10 W $m^{-2}$ $K^{-1}$ to 10.000 W $m^{-2}$ $K^{-1}$ from top to bottom and from left to right [44].

Oliet et al. [45] developed different models using different strategies for the simulation of dehumidifying tube-and-fin heat exchangers. According to the treatment of the heat conduction through the fins, three models were described: advanced model (AdvancedCHESS) of the multidimensional simulation, basic model (basicCHESS) based on the use of fin efficiencies, and quickCHESS based on enthalpy difference method (ε-NTU based model). AdvancedCHESS is a tube-by-tube model which allows determining of temperature fields over a discretized two-dimensional fin surface, convective heat transfer to air, fin efficiency, and liquid film formation and characteristics. These discretized quantities are then applied to relevant equations at the level of the macro-volumes formed by fin-and-tube. Experimental results from literature were used for a comparison of the simulation data with the tested one, showing a good agreement.

Based on graph theory, Liu et al. [46] created a universal steady-state model for a finned tube HX. Additionally, their model takes into account refrigerant distribution via complex circuitry layouts. The model starts with guessed wall temperatures as well as guessed outlet characteristics for air and refrigerant and applies conservation of energy to a specified control volume. Every control volume of the heat exchanger undergoes an iterative procedure to obtain the wall temperature, outlet refrigerant, and air parameters so that energy is conserved for each control volume.

A serious problem that affects heat exchangers operating at low temperatures is frost formation. Under certain operating conditions, when the humid air meets the cold HX surface below 0 °C, the frost that forms drastically worsens the exchanger performance by acting as a thermal resistance as well as reducing the air-flowing space, thus increasing the pressure drops. The first studies on frost growth were conducted by Niederer [47] and Kondepudi and O'Neal [48–50] who experimentally investigated the effect of frost formation on the overall performance, concluding that the heat exchangers with closer fins suffered a strong deterioration in performance compared to exchangers with a wider pitch, under frosting condition. In addition, different fin configurations were analyzed and compared. Other pure experimental studies were carried out by Seker et al. [51] and by Kim et al. [52] who investigated the thermal performance and frosting behavior accounting for different refrigerant flow arrangements (counter-flow and parallel-flow) and fin surface treatments (bare, hydrophilic, hydrophobic, and hybrid). Yan et al. [53] carried out experimental tests showing the overall heat transfer coefficient, variation of the heat transfer rate over time, and the pressure drops of single and multiple-row finned tube HXs under frosting conditions. More recent tests were performed by Zhang et al. [54], Reichl et al. [55], and Wu et al. [25]. The effects of frosting conditions on frost distribution and growth characteristics of HXs with different fin pitches were investigated by Zhang et al. [54], while Reichl et al. [55] compared hydrophobic nano-coated evaporators with uncoated ones with the use of a scale and image capturing techniques.

The analytical study of frost formation is quite complex, as it is a dynamic phenomenon that would require evaluation over time. Therefore, in most mathematical models the transient frost growth process is treated as a quasi-steady state phenomenon.

In one of the earliest analytical investigations, Lee et al. [56] created a model of a frost layer on a cold, flat surface by taking into account both heat production from the sublimation of water vapor in the frost layer and the molecular diffusion of water. Tso et al. [57,58], Yang et al. [59], and Padhmanabhan et al. [60] proposed valid models for HXs under frosting conditions with the weakness that they did not take into account the airflow reduction due to frost formation. On the other hand, the models by Ye and Lee [61], Silva et al. [62], Chen et al. [63], and Hwang and Cho [64] consider reducing the air flowrate by applying a pressure drop vs. volume flowrate curve. Hwang and Cho [64] proposed a model capable of calculating the blockage ratio (BR), frost thicknesses, and both local and total heat transfer rates by using a segment-by-segment method under both standard and high frosting conditions.

### *3.3. Small-Scale and Dynamic Models*

In this section numerical studies based on CFD techniques are selected and illustrated as well as a brief description of some time-dependent models is reported.

CFD codes are often employed to investigate the influence of geometrical parameters on the heat transfer and pressure drop characteristics of a chosen HX. A numerical investigation on a four-row finned tube HX with staggered/in-line tube arrangement and plain/wavy fins (Figures 10 and 11) was carried out by Bhuiyan and Islam [65] by using the commercial CFD code, ANSYS CFX-11, for laminar and turbulent flows and the k-ω turbulence model for transitional flow. Results showed that higher heat transfer performance could be achieved with wavy fins, if compared to plain fins (Figure 12). However, wavy fin configuration results in lower pressure drops (Figure 13). The model was validated by comparing the simulated case's friction factor, $f$, and Colburn factor, $j$, to experimental data

from literature [66,67], achieving maximum deviations of 10.22% and 11.25% for friction factor and Colburn factor, respectively.

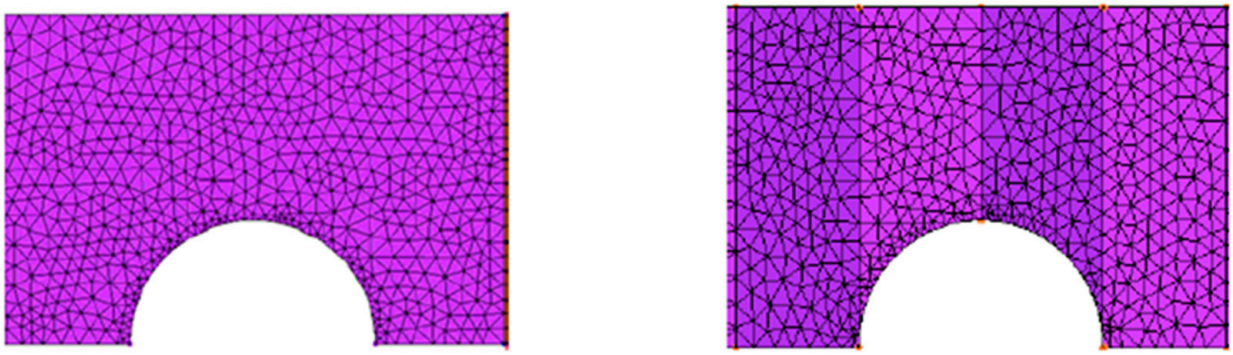

**Figure 10.** Surface mesh setup for plain and wavy fin configuration [65].

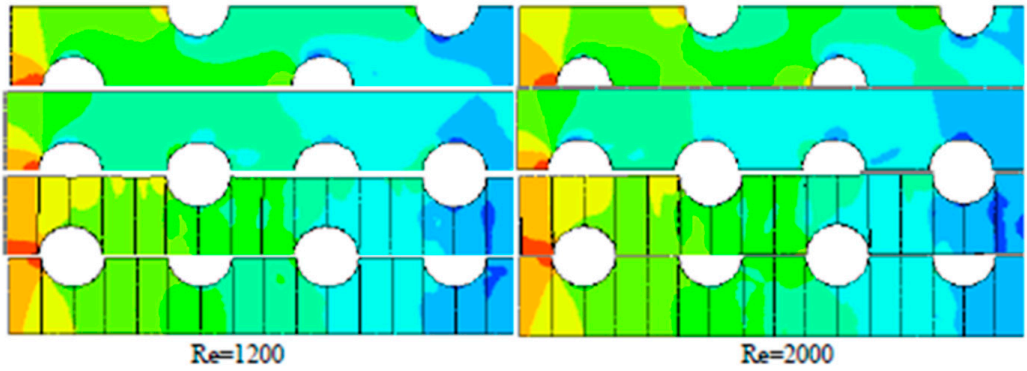


**Figure 11.** Pressure distribution for the fin configuration [65].

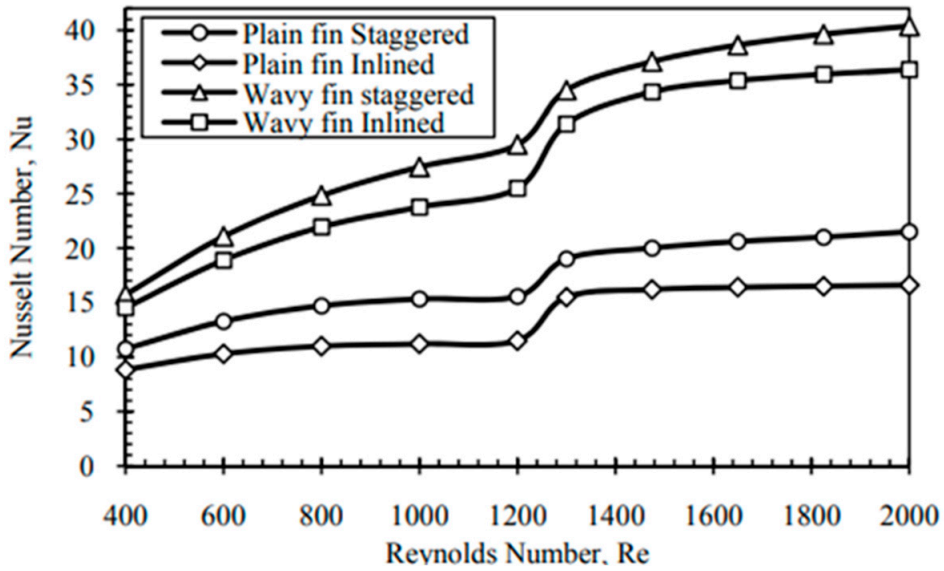


**Figure 12.** Nusselt number vs. Reynolds number for various fin configurations [65].

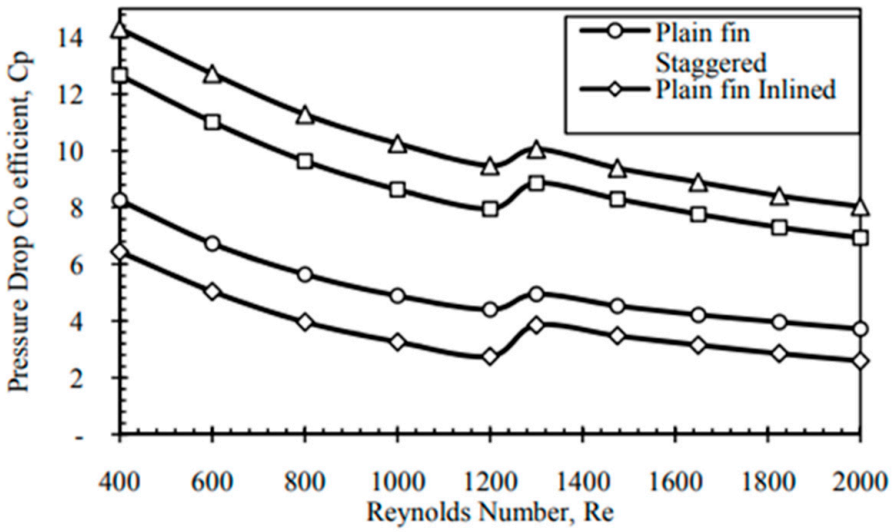


**Figure 13.** Impact on pressure drop coefficient for different fin configurations [65].

Recent works using CFD techniques mainly concern compound geometries or different fin profiles [68–70]. Lee et al. [68] performed an experimental and numerical analysis on wavy fin-and-tube heat exchangers with elliptic tubes and large waffle heights. The influence of different waffle heights, fin pitches, wave lengths, and inlet air velocities on thermo-fluid characteristics was analyzed with the use of CFD techniques and the model was then experimentally validated. In order to assess the effects of both the size and the form of fin perforations on heat transfer capabilities, Rauber et al. [69] computationally and experimentally evaluated heat exchangers with various fin patterns, i.e., rectangular with no insert and rectangular with diamond and circular perforations. According to the results, greater fin perforations—whether circular or diamond-shaped—improve both the PEC (performance evaluation criteria) parameter and the HX's thermal efficiency.

Additionally, Li et al. [70] concentrated on the impact of various geometric combinations (circle tube, ellipse tube, hexagon tube, rhombic tube, and fusiform tube). The hexagon tube had the best performance, according to the results, which also demonstrated that the wake region has a negative impact on heat transfer performance.

Fin efficiency was also studied by Lindqvist et al. [71] who performed numerical simulations to calculate correlations for pressure drops and air-side heat transfer for a wide variety of HX geometries. Different array angles and transverse tube array pitches were studied with the result that fin efficiency can be enhanced by minimizing the array angle.

Another recent study conducted by Taler et al. [72] aimed to develop a new method for determining the correlation for the Nusselt number on each pipe row in plate-finned tube HXs s using CFD modelling. The average heat transfer coefficient for each pipe row was calculated based on the comparison of the mass average air temperature increase, determined through CFD modelling and obtained by analytical correlation. The CFD technique was also employed to obtain correlations for the air-side Nusselt number. The same method was used by Taler et al. [73] to model a plate-finned tube heat exchanger under transient conditions.

CFD simulations were recently used to model frost formation and growth processes by Zhao et al. [74] who employed the impingement model to evaluate droplet formation based on Popovac et al.'s [75] work and by using an enthalpy porosity approach in order to describe the solidification problem. Results show that the frost growth process is highly influenced by the formation of droplets before nucleation and cannot be neglected in a model describing HXs' performance under frosting conditions.

Currently, there are few 3D numerical studies that have been conducted on finned tube HX, due to the complexity of the flow structure between the fins.

A study on 3D laminar and turbulent flows around tube banks was conducted by Zdravistch et al. [76]. Simulations for heat transfer predictions were performed on a tube bank without fins. Romero-Méndez et al. [77] performed a numerical investigation on the influence of fin spacing on heat transfer simulating a 3D 1-row plate-fin HX with Reynolds number in the range between 260 and 1640. Furthermore, Tutar et al. [78] studied the effect of fin spacing performing a three-dimensional numerical investigation over a single row tube domain, for a Reynolds number range between 1200 and 2000.

Other authors focused on the study of transient phenomena related to heat exchange by developing time-dependent models. Zhang and Zhang [79] described the transient behavior of dry-expansion evaporators through a moving boundary approach with a time-variant mean void fraction—instead of constant—in order to improve the robustness of the traditional moving-boundary models. With the aim to obtain the mean properties in the two-phase region and the superheated zone, numerical integration was also used. Furthermore, Willatzen and Pettit [80,81] proposed a mathematical model to describe the transient phenomena of two-phase flow heat exchangers. The three zones (liquid, two-phase, and vapor) present in the HX are integrated separately to generate a series of ordinary-differential equations that make up the model.

Shao and Zhang [82] focused on the dynamic variation of the number of zones of an evaporator or condenser (Figure 14), due to disturbance or oscillation in operating conditions. For instance, the superheated region in the evaporator can shorten or eventually vanish with the increase in the mass flow rate. Therefore, they developed a logic-unconstrained multi-zone model to describe the zone's variation, where the traditional constraints were removed and substituted with continuously differentiable equations.

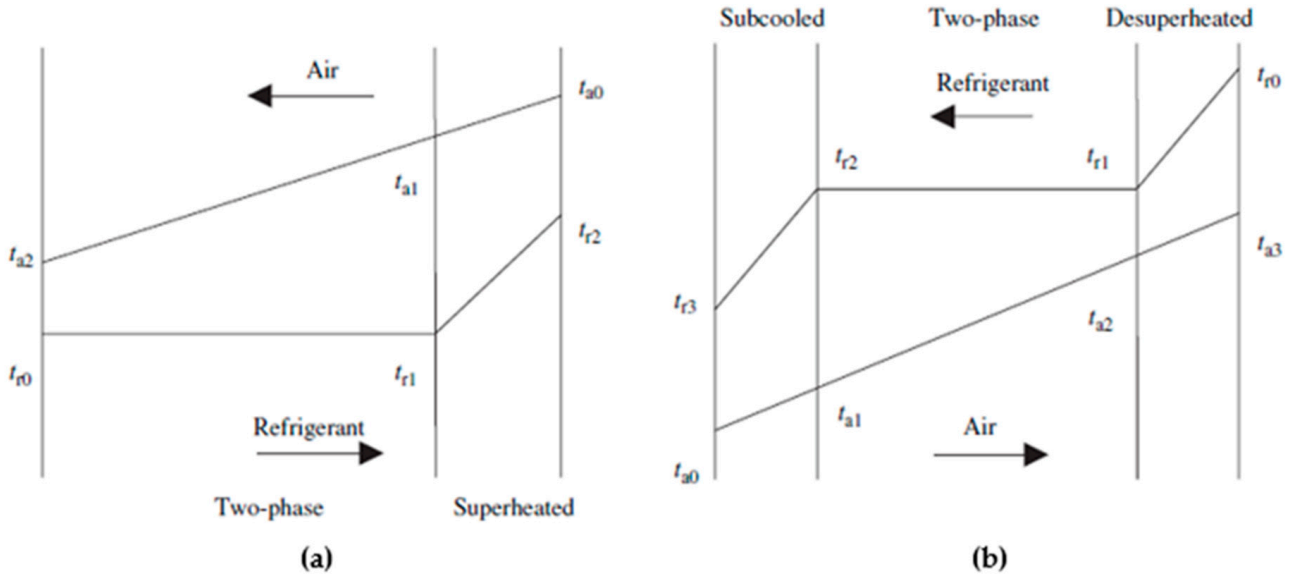


**Figure 14.** Temperature distribution of a counter flow evaporator (**a**) and condenser (**b**) [82].

Recently, Illàn-Gmez et al. [83] developed a model based on the exchanger's one-dimensional discretization that enables the solution of the heat transfer balance equations using an iterative process based on the heat transfer area converging criterion. The numerical method has been proven to be reliable and has been applied to forecast the evaporator's performance in transient operating conditions, with a high degree of accuracy.

### *3.4. Multi-Scale Models*

Multi-scale models require a good knowledge of all modeling methods previously described. Generally, they are very flexible and suitable for different HX geometries and working conditions because they integrate analytical methods' benefits with more precise numerical approaches.

The hybrid method is an alternative design procedure developed by Starace et al. [84] and based on an algorithm that uses a multi-scale method, based on data from either analytical, numerical, or experimental investigations. The hybrid approach was originally used on compact cross-flow HXs, where the entire geometry was split into a number of control volumes, each of which had a warm side and a cold side. Through the application of a regression technique, Carluccio et al.'s [85] thermo-fluid dynamics simulation findings on the two finned surfaces of the HXs were used to develop the prediction functions of heat transfer, extending the local results over the whole geometry of the HX.

By starting with small-scale experimental tests, Fiorentino and Starace [86] developed another application of the hybrid technique for countercurrent evaporative condensers to assess their performance. Results indicate that, when compared to experimental tests, the method is accurate and can determine the air temperature and relative humidity at the output with errors of 2.5% and 4%, respectively.

Then, Starace et al. [87] employed this technique on a plate-finned evaporator with a basic refrigerant circuit configuration, using the control volume approach (Figure 15). The heat transfer rate decreases from a maximum of 0.88 W in the first row to 0.38 W in the last row, where the refrigerant does not achieve evaporation as in the first row. Wall temperature distribution through the evaporator was also obtained as a result (Figure 16).

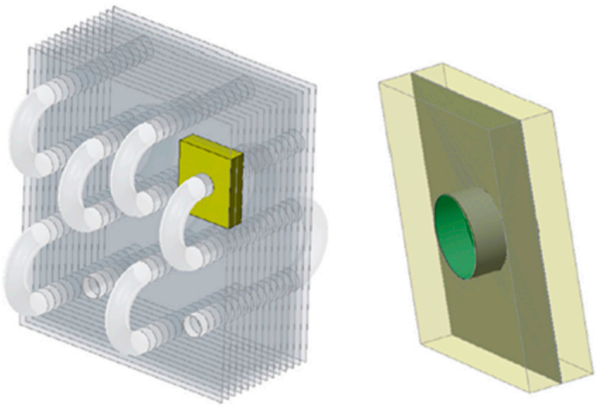

**Figure 15.** Elementary control volume on the refrigerant side (green, **right side**) and the air side (yellow, **left side**) [87].

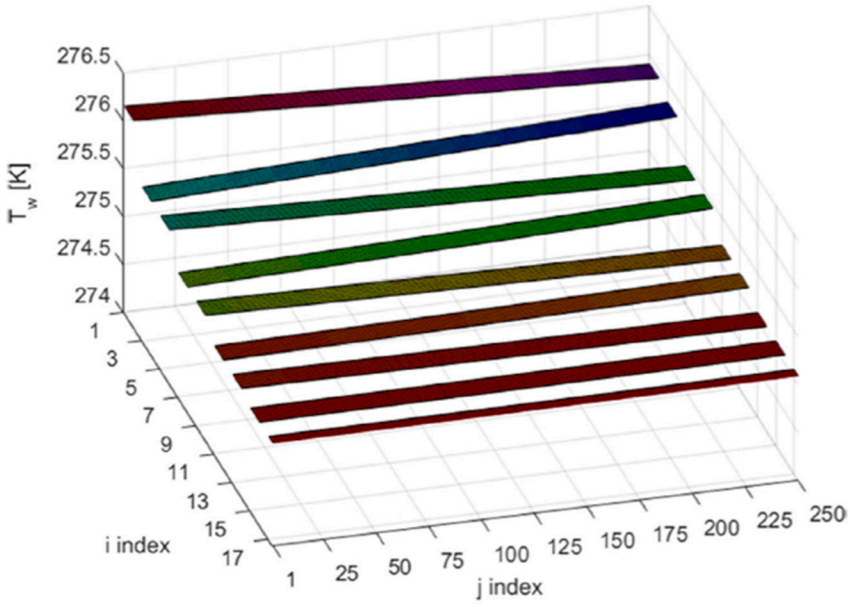


**Figure 16.** Wall temperature distribution in the HX first row [87].

Starace et al. [88] achieved progress in the development of the hybrid technique by using it on evaporators with complex circuit layouts (Figure 17) to assess the impact of circuitry configuration on overall performance in terms of heat transfer rate and refrigerant pressure drops. Also in this study, the whole HX's geometry was schematized through a three-dimensional matrix with the position of each cell identified by the indices *i*, *j* and *k* (Figure 18). According to the results, the heat transfer rate and pressure drops reduce significantly as the number of circuits rises; as a result, installation costs will rise and operation costs will decrease.

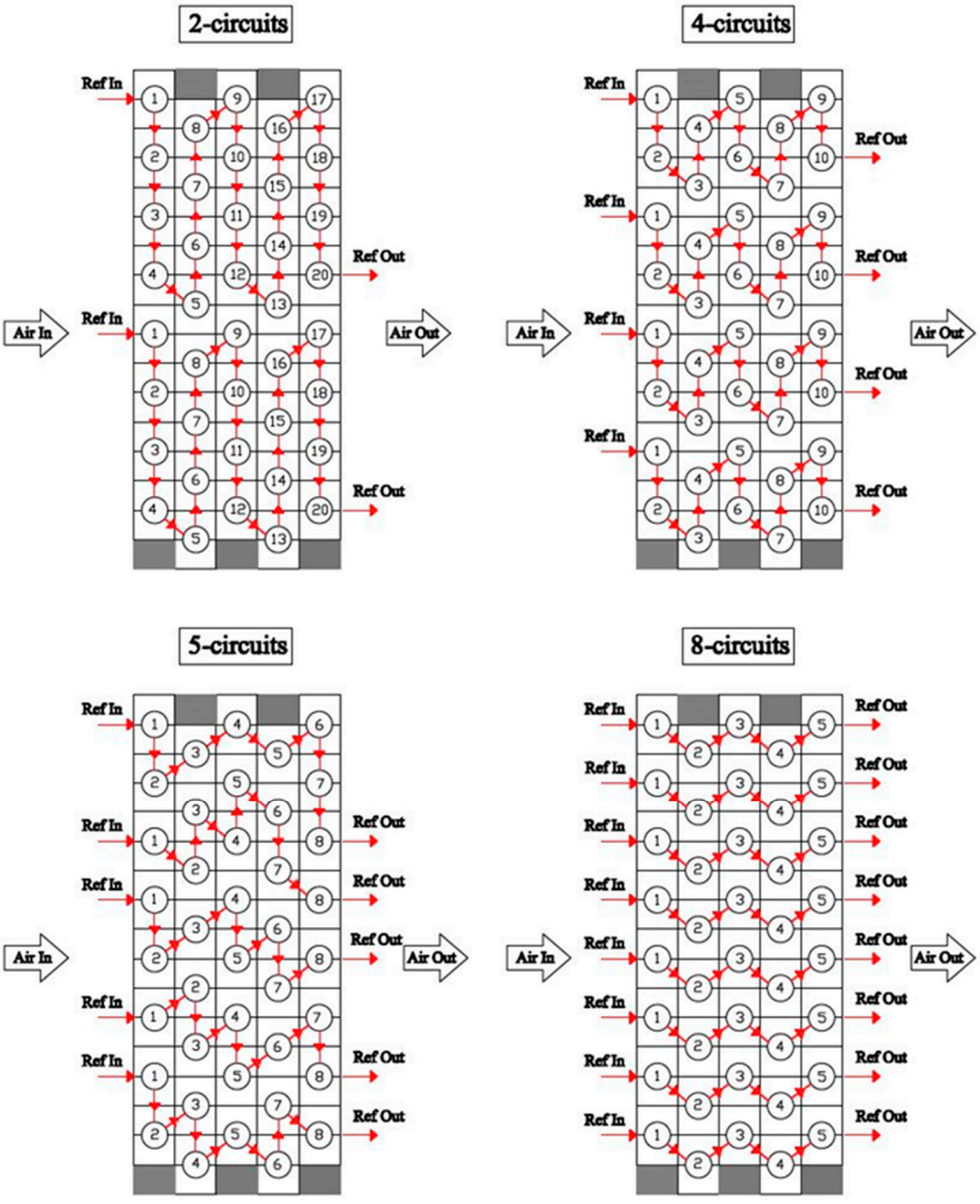


**Figure 17.** Tested circuitry layouts [88].

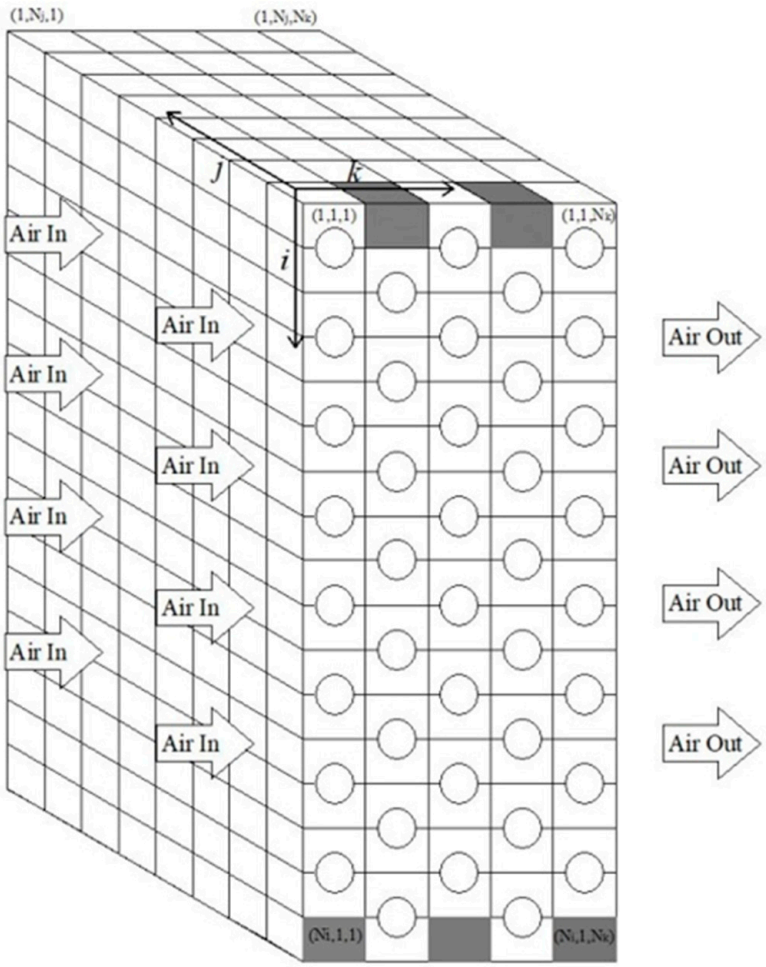


**Figure 18.** The scheme of the HX's geometry through a three-dimensional matrix [88].

Then, additional tests were conducted while taking into account various refrigerants and changing the fluid conditions at the input [89]. The findings demonstrate that all investigated refrigerants (R134a, R410a, R507a, R32, R404a, R1234ze, and R1234yf) act similarly when the number of circuits is varied.

Other investigations using R134a on various circuitry configurations revealed that an eight-circuit layout can be used to lower the refrigerant pressure drop of 45.3% and consequently operating costs by increasing the refrigerant flowrate of 314% while keeping the same performance in terms of heat transfer rate. More research performed on several circuitry layouts revealed that the air inlet side has no discernible impact on the heat transfer rate performance of the HX [89]. Other studies also showed that it is possible to optimize the refrigerant path while maintaining the same number of circuits, but the advantage in terms of improved performance is minimal [89].

The hybrid approach algorithm underwent additional modifications to make it even more adaptable and compatible with predictions of the performance of real heat exchangers [90].

Other tests were conducted by adjusting the operating conditions, such as the temperature gradient between refrigerant and air at the inlet and the air relative humidity. Part of the algorithm code was so altered in order to broaden the model's application range. According to the results, a larger value of air relative humidity at the intake can improve performance in terms of heat transfer rate as well as an increase in refrigerant pressure drops. Additionally, raising the temperature difference between the working fluids can enhance the heat transfer rate but degrade refrigerant pressure drop performance. Moreover, the simulation results revealed that at higher relative humidity, one additional degree

of temperature difference at the intake had a bigger impact on both the heat transfer rate and pressure drops. Comparing the tests, higher air temperature yields better performance than lower refrigerant temperature at the same temperature difference because there are less refrigerant pressure drops at the same heat transfer rate.

A selection of the reviewed models can be found in Table 3.

**Table 3.** A selection of finned tube modelling methods.

| Author | HX Configuration and Features | Simulation Tool/ Method Approach | Deviation between Simulated and Experimental Data | Ref. |
|---|---|---|---|---|
| Corberan et al. | - Finned tube evaporator/condenser | Control volume approach | +3.5%; −3% for evap. capacity<br>−5.5% for cond. capacity<br>12%; −8.5% for degree of superheat<br>−3% for degree of subcooling<br>15% evaporator pressure drops | [32,33] |
| Jiang et al. | - Air-to-refrigerant HX<br>- Complex circuitry configuration<br>- Multiple refrigerants<br>- Non-uniform air distribution | CoilDesigner<br>Segment-by-segment approach | ±10% (comparing with exp. data from [35]) | [34] |
| Tarrad and Al-Nadawi | - Louvered finned tube evaporator<br>- Pure and zeotropic blend refrigerants | Tube-by-tube approach | −7%; +1% for heat duty<br>−25%; +12% for outlet air temperature | [36] |
| Joppolo et al. | - Finned tube condenser<br>- Complex circuitry configuration | Control volume approach | ±5% for heat transfer rate<br>±21% for refrigerant pressure drop | [37] |
| Tong et al. | - Finned tube evaporator | Control volume approach | ±3% for cooling capacity<br>±0.2% for refrigerant evaporation temperature | [38] |
| Domanski | - Finned tube evaporator<br>- Complex circuitry configuration<br>- Non-uniform air distribution | Tube-by-tube approach | Percentage data not available | [39,40] |
| Bensafi et al. | - Single-phase HX/evaporator/condenser<br>-Water, R22, R134a and mixtures based on R32, R125, and R134a<br>- Complex circuitry configuration<br>-Plain/wavy/louvered fins<br>- Smooth and internally finned tubes | CYRANO<br>Control volume approach | ±5% for heat duty<br>±30% for pressure drops | [41] |
| Liang et al. | - Evaporator<br>- Complex circuitry layout | Control volume approach | ±5% for heat duty<br>±25% for pressure drops | [42] |
| Ding et al. | - Evaporator | analytical-experimental approach | ±8% for heat transfer rate | [43] |
| Singh et al. | - Air-to-refrigerant HX<br>- Temperature distribution on fin surface | Segment-by-segment approach | ±3%–±5% for overall heat load<br>±3.9 °C for tube-bend temperatures | [44] |
| Oliet et al. | - Dehumidifying finned tube HX | - QuickCHESS (ε-NTU method)<br>- BasicCHESS<br>- AdvancedCHESS (control volume approach) | ±10% for cooling capacity<br>±10% for water vapor condensate<br>±25% for air pressure drop<br>±25% for liquid pressure drop | [45] |
| Liu et al. | - Finned tube HX<br>- Complex circuitry layout | Control volume approach | ±10% for heat transfer rate<br>±20% for pressure drop | [46] |
| Bhuiyan and Islam | - Staggered/in-lined<br>- wavy/plain fins<br>- one-phase flow | ANSYS CFX-11, k-ω model for transitional flows | Comparing with exp. data from [66,67]:<br>+10.22% for friction factor<br>+11.25% for Colburn factor | [65] |
| Zdravistch et al. | - Tube banks without fins | 3D simulation (laminar and turbulent flow) | - | [76] |
| Romero-Méndez et al. | - 1-row plate-finned tube HX<br>- Different fin space | 3D simulation<br>($260 \leq Re \leq 1640$) | - | [77] |
| Tutar et al. | - 1-rowplate-fin HX<br>- Different fin space | 3D simulation<br>($1200 \leq Re \leq 2000$) | - | [78] |
| Zhang and Zhang | - Evaporator | Transient simulation<br>Moving boundary approach | - | [79] |
| Willatzen et al.<br>Pettit et al. | - Evaporator/condenser | Transient simulation | - | [80,81] |
| Shao and Zhang | - Evaporator/condenser | Transient simulation Logic unconstrained multi-zone model | - | [82] |
| Illan-Gomez et al. | - Evaporator | Transient simulation segment-by-segment approach | ±10% for heat transfer rate<br>±10% for refrigerant inlet pressure<br>±2 °C for refrigerant inlet temperature<br>±1 °C for refrigerant outlet temperature | [83] |
| Starace et al.<br>Fiorentino et al. | - Evaporator/condenser/crossflow compact HX<br>- Complex circuitry layout | Control volume approach<br>Multi-scale model | ±3% for outlet temperature<br>±4% for outlet relative humidity | [84,86–90] |

## 4. Heat Exchanger Optimization Methods

The optimization process of a finned tube HX can be very complex, due to the high number of design variables. Optimizing the refrigerant path by modifying circuit arrangement is the best method for cost saving, compared with other optimization procedures, such as change of fin or tube geometry or the overall dimensions, as discussed by Yun and Lee [91] and Matos et al. [92], due to constraints that often occur in small installation spaces or dealing with manufacturing issues. For instance, distributing the refrigerant flow across multiple circuits can be a good way to reduce refrigerant pressure drops and thus optimizing the design.

Some authors studied the influence of the refrigerant circuit layout by performing tests with different circuitry arrangements, such as Joppolo et al. [37] who carried out a numerical analysis on a fin and tube condenser, calculating the heat transfer rate between air and refrigerant with the ε-NTU method for each element which the condenser geometry was divided into.

Starace et al. [88,89] ran different simulation tests on an evaporator, on some sets of circuitry layouts, considering the heat transfer rate and refrigerant pressure drop, and then building trade-off curves to help designers to choose the best circuit configuration (Figure 19).

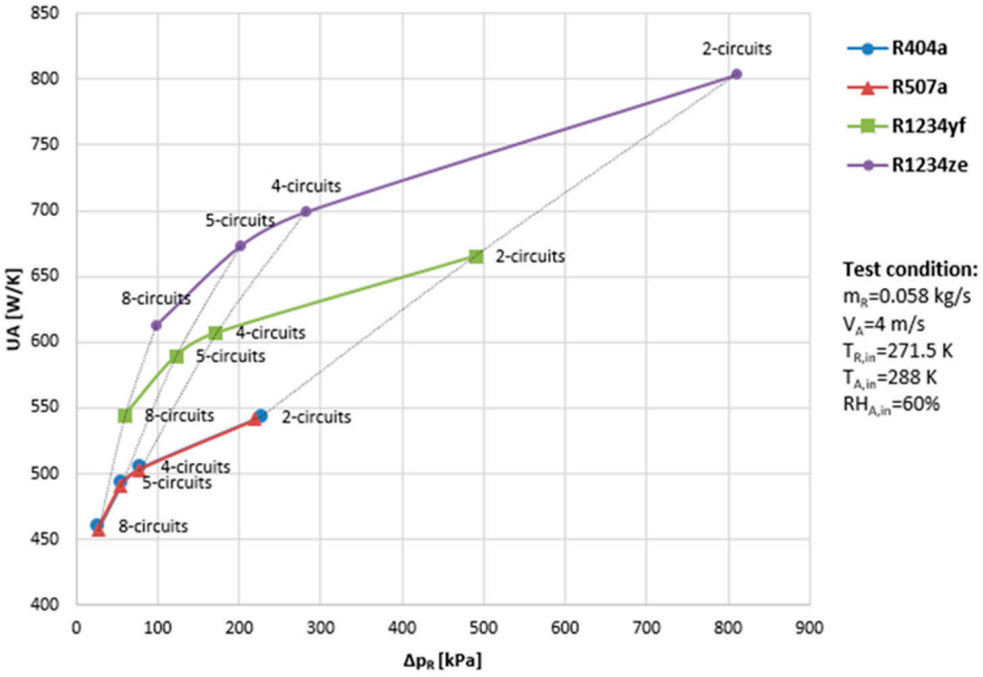


**Figure 19.** Impact of number of circuits on UA factor and refrigerant pressure drop for refrigerants R507a, R404a, R1234yf, and R1234ze [89]. The gray lines represent the junctions between points with the same number of circuits.

Another research that accounted for refrigerant pressure drop in order to optimize the circuitry arrangement was carried out by Wang et al. [93], who conducted an experimental study on different circuitry configurations on wavy fin condensers. The counter-cross arrangement obtained the best performance. Similar studies were then performed by Ding et al. [94] for condensers and Liang et al. [42] for evaporators. Ding et al. [94] performed simulations on a condenser, where the refrigerant flow is divided into four branches at the entrance, and the four branches are then combined to form one main channel to the exit (Figure 20). Different branches are identified by blue/red colors in Figure 21, which displays the simulation results in terms of refrigerant pressure drop and tube heat transfer capacity. It is easy to see how the main channel and branches perform differently. The four branches are expected to have similar refrigerant flowing conditions, because they all have

the same number of tubes and equivalent paths, as shown by the nearly identical pressure drop distribution in Figure 21a. Reasonable outcomes for the heat transfer aspect are also displayed in Figure 21b where the main differences in performance are due to the specific location of the tubes with respect to the air flows.

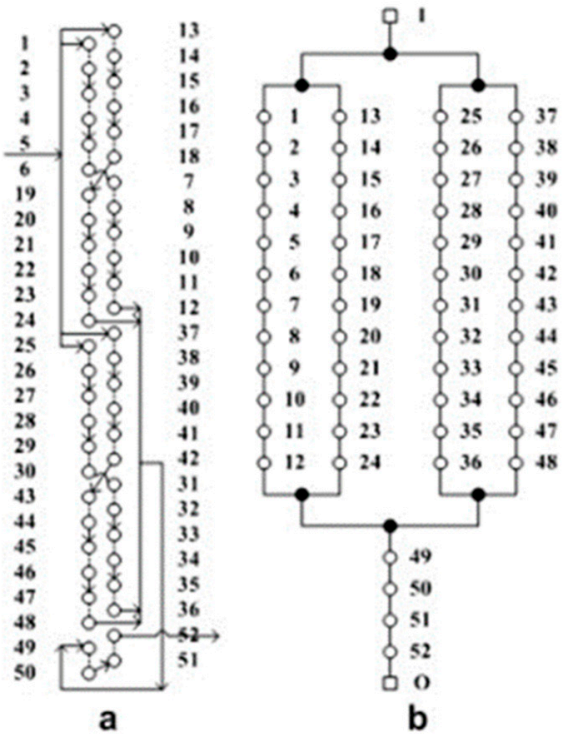


**Figure 20.** Circuitry layout (**a**) and connection map (**b**) for simulated condenser [94].

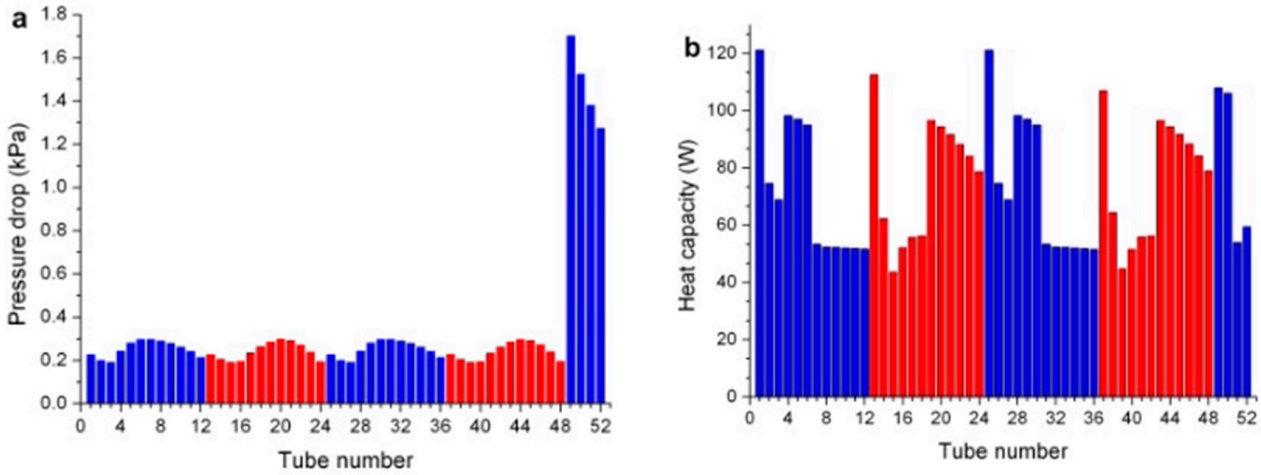


**Figure 21.** Results for the simulated condenser in terms of pressure drop (**a**) and heat capacity (**b**) [94].

Through a segment-by-segment model validated through experimental tests, Saleem et al. [95] investigated how refrigerant circuitry can affect cross-fin conduction in evaporators with multiple circuits. Results demonstrated that the influence of cross-fin conduction on coil capacity is increased in HX with interleaved circuitry operating at partial loads as opposed to being minor when all refrigerant circuits are active or some are blocked. Bach et al. [96] focused instead on optimization methods for the mitigation of air maldistribution, showing how interleaved circuitry can reduce the effects of air maldistribution if paired circuits are chosen properly.

An attempt to optimize the circuit layout was made by Cen et al. [97] who developed a simple method to automatically generate different refrigerant circuitry arrangements for finned-tube HXs, based on an iterative procedure. Then, a simulation for HX performance prediction calculates the heat transfer rate that allows the designer to choose among the tested layouts. However, since the model states that a tube is only linked to those in its neighborhood, only part of the potential arrangement options are taken into account, so there is no guarantee that the found layout represents the global optimal solution.

Other authors, instead, focused on researching intelligent systems for circuit optimization, developing genetic algorithms or simulation tools considering the maximum value of heat exchanger capacity [98–102], the minimum value of heat transfer surface with the same heat transfer rate [101,102], or the minimum generation of entropy [103,104]. The missing information from these studies is the influence of circuitry layout on the pressure drop, which is useful for reducing operating costs.

Finding an optimization technique becomes a problem of great important since there are an increasingly huge number of circuit designs that can be made with a given number of tubes. The standard genetic algorithms (GA) consider the initial set of possible solutions as a population of individuals with different genetic features (i.e., strings of instructions that encode a possible solution to the problem). With appropriate methods of crossing and replication, these individuals generate other solutions; a mechanism of mutation and natural selection ensures that the best solutions prevail in the reproductive process and ultimately determine the success of the species in solving the given problem.

These algorithms are relatively easy to apply [105] but need to be improved, due to the complicated nature of circuitry layout optimization. An improved genetic algorithm (IGA) together with a knowledge-based evolution method (KBEM) was developed by Wu et al. [101,102]. Additionally, the inclusion of correction operators allowed for the avoidance of impractical solutions without reducing the search space, and the introduction of a novel refrigerant circuit representation allowed for the reduction of both computer memory usage and decoding time. The authors ran some case studies showing that KBEM with IGA can generate circuitry layouts more efficiently than only IGA by reducing the search space, according to the domain knowledge.

An integer permutation-based genetic algorithm (IPGA) was created by Li et al. [106] for optimizing circuitry under manufacturability and operating restrictions. All of the chromosomes produced by IPGA can be sorted using the genetic operators in a valid circuit layout (Figure 22). As a consequence, this method can efficiently search the solution space compared to traditional GA (Figure 23. Manufacturability constraints are managed in the fitness assignment step using a constraint-dominated sorting technique (Figure 24).

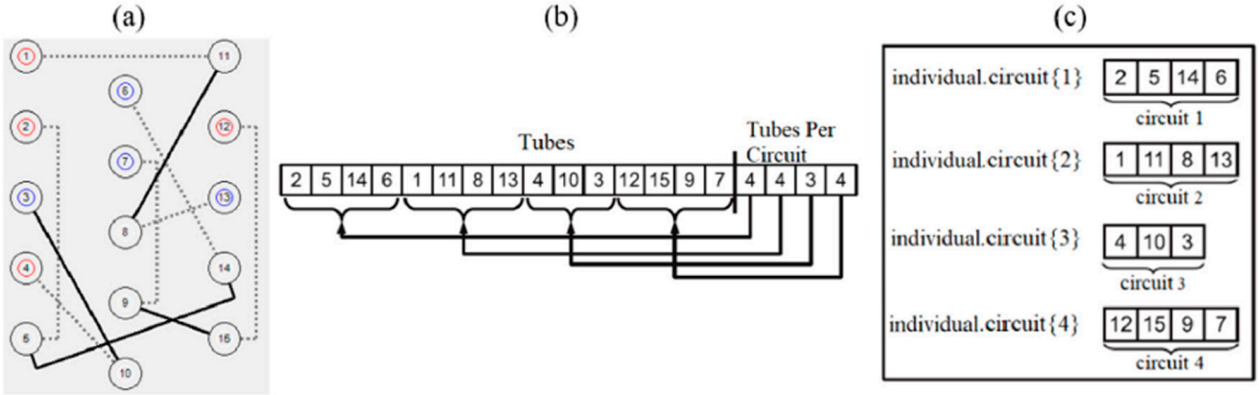


**Figure 22.** Scheme of circuitry layout: (**a**) 15-tube HX; (**b**) two-part chromosome; (**c**) split circuit chromosome [106].

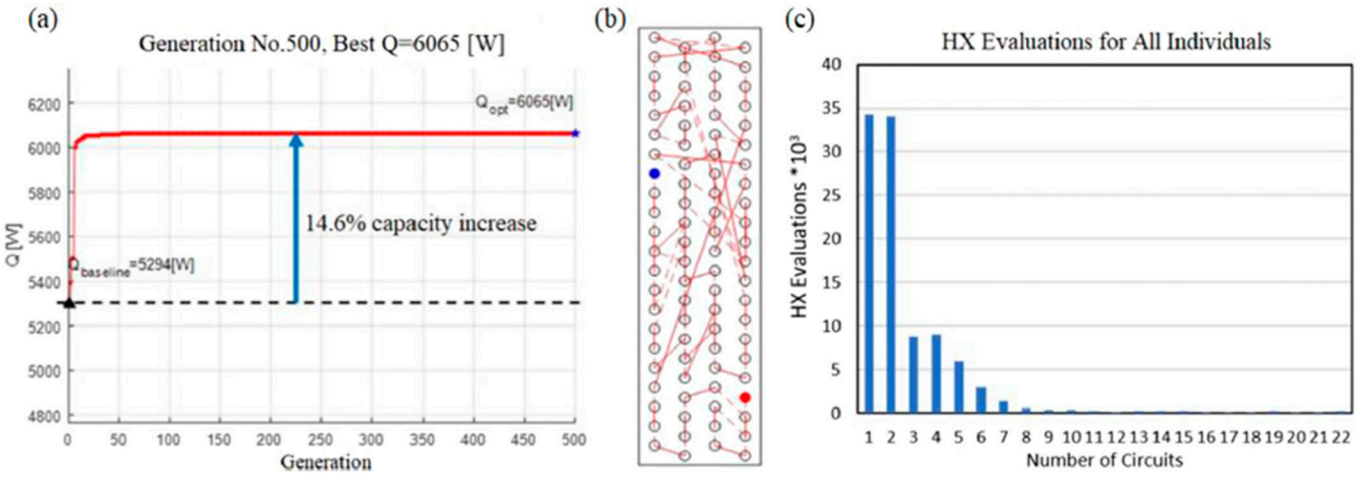


**Figure 23.** (**a**) Optimal circuitry configuration; (**b**) GA optimization process; (**c**) histogram of number of circuits [106].

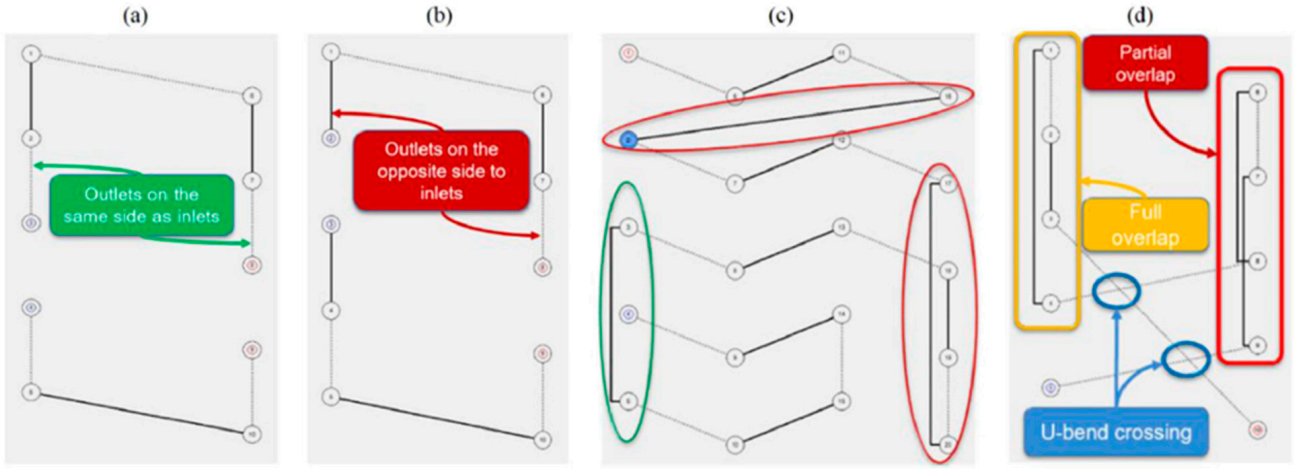


**Figure 24.** Manufacturing restrictions: (**a**) outlets on the same side as inlets; (**b**) outlets on the opposite side to inlets; (**c**) long bends; (**d**) different kinds of bend crossovers [106].

A genetic algorithm was also used by Gholap and Khan [107] to solve the multi-objective optimization of an HX for refrigerators, accounting for different design variables (Figure 25). Two objectives were considered for the analysis: minimization of energy consumption and material cost. Since these objectives are conflicting, no single design was found to satisfy both criteria simultaneously. Therefore, a set of multiple optimum solutions, called 'Pareto optimal solutions', were given as the output of the study.

Ploskas et al. [108] applied a group of five derivative-free optimization (DFO) algorithms to search for the optimal or near-optimal solution of the HX circuitry arrangement. By treating the refrigerant circuitry design process as a constrained binary optimization problem, they presented a novel formulation for the process. Results of using DFO solvers on 17 heat exchangers demonstrated that the suggested techniques produce optimal or nearly optimal circuit designs without necessitating in-depth domain knowledge.

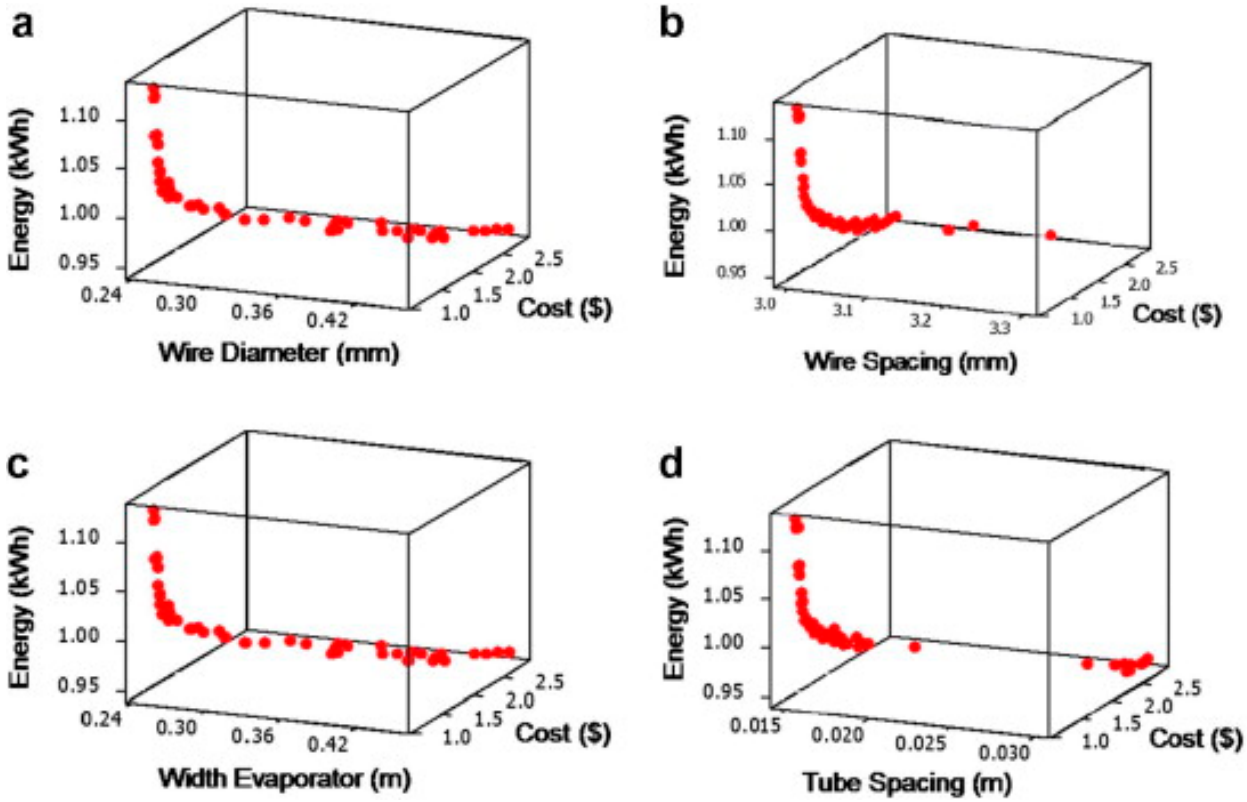


**Figure 25.** Design variables' impact such as wire diameter (**a**), wire spacing (**b**), width evaporator (**c**) and tube spacing (**d**) on design criteria within optimal solutions [107].

A more recent optimization study, carried out by Ishaque and Kim [109], involves a dual-mode algorithm for searching the refrigerant circuitry optimal solution. A first knowledge-based computational module (KBCM) establishes the optimal number of circuits also accounting for non-uniformity air distribution at the inlet, while the output of the permutation-based computational module (PBCM) determines the optimal tube sequence that allows the maximization of the exchanger heat capacity. A multi-objective optimization was performed by Dehaj and Hajabdollahi [110], who modeled and optimized a fin and tube heat exchanger, in order to increase effectiveness while minimizing the total annual cost (TAC) by modifying eight design variables for each section. Furthermore, in this case, a genetic algorithm was implemented to find the optimal Pareto front.

A very recent study on an exchanger with improved fin geometry (vortex generators) was performed by Xie et al. [111] using the response surface methodology (RSM) and artificial neural network (ANN), in order to improve flow and heat transfer characteristics (Nusselt number and friction factor). First, a numerical model that took into account the vortex generator's length, arc angle, and attack angle, was created. Then, two RSM models and two ANN models were trained to individually estimate the Nusselt number and friction factor for each of the 15 design configurations, chosen with the help of a central composite design approach (CCD).

## 5. Conclusions, Future Trends and Recommendations

In this paper, the modeling methods for calculating the performance of plate-finned tube heat exchangers have been selected and reviewed in order to propose a classification by scale of approach and to help designers to choose the most suitable design method compatible with market demands in terms of performance and costs. Furthermore, several optimization methods have been described, with a focus on the refrigerant circuitry configurations, being one of the most important factors affecting the performance of the

exchangers. Below some considerations that followed from the study of the models are reported, together with some suggestions for future research:

- In the last couple of years, research has focused above all on the study of the fluid-dynamic and thermal characteristics of the exchangers through the use of CFD techniques [68–73]. Several experimental tests were also carried out for the same purpose [22–28], but in order to save time and resources, it is recommended that research goes even deeper into cost-saving methods—without loss of accuracy—such as multi-scale models for the prediction of performance.
- Greater accuracy in predicting pressure drops would be appreciable in future research. Most of the analytical models analyzed here showed a good agreement of the simulated data with the experimental tests in terms of heat capacity, but failed to predict pressure losses as effectively (deviation was found between 15% and 30%).
- A good design is often penalized by unexpected working conditions, such as non-uniform air distribution at the inlet or refrigerant maldistribution, due to blocked or partially clogged tubes, which significantly degrade performance. Some studies were performed in the past to predict the exchanger behavior in real operating conditions, but further investigation needs to be carried out in the future.
- Future research studies should also include the superheat region for evaporators and subcooling for condensers as these operating zones often occur in practice.
- Performance prediction of HXs under frosting conditions is very complex as it is a dynamic phenomenon that leads to a drastic worsening of performance. In order to develop more accurate frosting analytical models, it is recommended that future studies will focus on this research area.
- A research path that has been developing in recent years concerns the modeling of heat exchangers with improved and compound fin geometries, such as fins with diamond or circular perforations and vortex generators as well as new tube shapes (rhombic, hexagon, etc.). Further developments in this research area are desirable since the results obtained in terms of performance improvement are encouraging.
- Recently, very interesting experimental studies [27,28] showed that the performance of a reversible heat pump can be enhanced by means of different circuitry arrangements for the exchanger whether it is used as an evaporator or condenser. These studies can be the basis to make progress in developing new computational and optimization models for heat exchangers with reversely-variable circuitry.

**Author Contributions:** Conceptualization, G.S. and G.C.; methodology, G.S.; software, S.M.; validation, G.S., G.C. and S.M.; formal analysis, G.S., G.C. and S.M.; investigation, G.S., G.C. and S.M.; writing—original draft preparation, G.S., G.C. and S.M.; writing—review and editing, G.S., G.C. and S.M.; supervision, G.S. and G.C. All authors have read and agreed to the published version of the manuscript.

**Funding:** This research received no external funding.

**Data Availability Statement:** The data presented in this study are available on request from the corresponding author.

**Conflicts of Interest:** The authors declare no conflict of interest.

## Nomenclature

| | |
|---|---|
| $D$ | tube diameter (m) |
| $D_h$ | hydraulic diameter (m) |
| $f$ | friction factor |
| $J$ | Colburn factor |
| $L$ | tube length (m) |
| $N_R$ | number of tube rows |
| $Nu$ | Nusselt number |
| $\overline{Nu}$ | average Nusselt number |

Abbreviations

| | |
|---|---|
| *ANN* | artificial neural network |
| *CCD* | central composite design method |
| *CFD* | computational fluid dynamics |
| *CHX* | compact heat exchanger |
| *COP* | coefficient of performance |
| *DFO* | derivate-free optimization |
| *FTHX* | finned tube heat exchanger |

| | | | |
|---|---|---|---|
| $Nu_z$ | Nusselt number by Zukauskas correlation | *GA* | genetic algorithm |
| $P_F$ | fin pitch (m) | *HTC* | heat transfer coefficient |
| $P_L$ | longitudinal pitch (m) | *HX* | heat exchanger |
| *Pr* | Prandtl number | *IGA* | improved genetic algorithm |
| $P_T$ | transverse pitch (m) | *IPGA* | integer permutation-based genetic algorithm |
| *Re* | Reynolds number | *KBCM* | knowledge-based computational module |
| *Sh* | Sherwood number | *KBEM* | knowledge-based evolution method |
| Greek symbols | | *NTU* | number of transfer units |
| $\varepsilon$ | heat transfer effectiveness | *PBCM* | permutation-based computational module |
| | | *RSM* | response surface method |

## References


1. Bergman, A.A.; Incropera, F.P. *Fundamentals of Heat and Mass Transfer*; John Wiley & Sons: Hoboken, NJ, USA, 2011.
2. Rohsenow, W.M.; Hartnett, J.P.; Cho, Y.I. *Handbook of Heat Transfer*, 3rd ed.; McGraw-Hill: New York, NY, USA, 1998.
3. Tahseen, T.M.; Ishak, M.; Rahman, M.M. An overview on thermal and fluid flow characteristics in a plain plate finned and un-finned tube banks heat exchanger. *Renew. Sustain. Energy Rev.* **2015**, *43*, 363–380. [CrossRef]
4. Basavarajappa, S.; Manavendra, G.; Prakash, S.B. A review on performance study of finned tube heat exchanger. *J. Phys. Conf. Ser.* **2020**, *1473*, 012030. [CrossRef]
5. Kakac, S.; Liu, H. *Heat Exchangers: Selection, Rating and Thermal Design*, 2nd ed.; CRC Press: Boca Raton, FL, USA, 2002.
6. Hesselgreaves, J.E.; Law, R.; Reay, D. *Compact Heat Exchangers: Selection, Design and Operation*, 2nd ed.; Butterworth-Heinemann: Oxford, UK, 2016.
7. Zohuri, B. *Compact Heat Exchangers*, 1st ed.; Springer: Cham, Switzerland, 2017.
8. Klemes, J.J.; Arsenyeva, O.; Kapustenko, P.; Tovazhnyanskyy, L. *Compact Heat Exchangers for Energy Transfer Intensification: Low Grade Heat and Fouling Mitigation*, 1st ed.; CRC Press: Boca Raton, FL, USA, 2015.
9. Wang, C.-C.; Hwang, Y.-M.; Lin, Y.-T. Empirical correlations for heat transfer and flow friction characteristics of herringbone wavy fin-and-tube heat exchangers. *Int. J. Refrig.* **2002**, *25*, 673–680. [CrossRef]
10. Shah, R.K.; Sekulic, D.P. *Fundamentals of Heat Exchanger Design*; John Wiley & Sons: Hoboken, NJ, USA, 2003.
11. Cain, J.W. Mathematical Models in the Sciences. In *Molecular Life Sciences*; Bell, E., Ed.; Springer: New York, NY, USA, 2014; pp. 1–6.
12. Colburn, A.P. A method of correlating forced convection heat-transfer data and a comparison with fluid friction. *Int. J. Heat Mass Transf.* **1964**, *7*, 1359–1384. [CrossRef]
13. Rosman, E.; Carajilescov, P.; Saboya, F. Performance of one-and two-row tube and plate fin heat exchangers. *J. Heat Transf.* **1984**, *106*, 627–632. [CrossRef]
14. Dittus, F.; Boelter, L. Heat transfer in automobile radiators of the tubular type. *Int. Commun. Heat Mass Transf.* **1933**, *12*, 3–22. [CrossRef]
15. Merker, G. Heat transfer and pressure drop on the shell-side of tube-banks having oval-shaped tubes. *Int. J. Heat Mass Transf.* **1986**, *29*, 1903–1909. [CrossRef]
16. Wang, C.-C.; Lee, W.-S.; Sheu, W.-J. Airside performance of staggered tube bundle having shallow tube rows. *Chem. Eng. Commun.* **2001**, *187*, 129–147. [CrossRef]
17. Žukauskas, A. Heat Transfer from Tubes in Crossflow. *Adv. Heat Transf.* **1972**, *8*, 93–160.
18. Kim, Y.; Kim, Y. Heat transfer characteristics of flat plate finned-tube heat exchangers with large fin pitch. *Int. J. Refrig.* **2005**, *28*, 851–858. [CrossRef]
19. Khan, M.G.; Fartaj, A.; Ting, D.S.-K. Study of cross-flow cooling and heating of air via an elliptical tube array. *ASHRAE Trans.* **2005**, *111*, 423–433.
20. Paeng, J.; Kim, K.; Yoon, Y. Experimental measurement and numerical computation of the air side convective heat transfer coefficients in a plate fin-tube heat exchanger. *J. Mech. Sci. Technol.* **2009**, *23*, 536–543. [CrossRef]
21. Taler, D. Experimental determination of correlations for average heat transfer coefficients in heat exchangers on both fluid sides. *Heat Mass Transf.* **2013**, *49*, 1125–1139. [CrossRef]
22. Okbaz, A.; Pınarbaşı, A.; Olcay, A.B. Experimental investigation of effect of different tube row-numbers, fin pitches and operating conditions on thermal and hydraulic performances of louvered and wavy finned heat exchangers. *Int. J. Therm. Sci.* **2020**, *151*, 106256. [CrossRef]
23. Bozkula, G.; Demir, H. Experimental investigation of heat transfer and pressure drop of fin and tube heat exchanger under dry and wet conditions. *Int. J. Therm. Sci.* **2022**, *177*, 107580. [CrossRef]
24. Wu, W.; Luo, J.; Li, D.; Feng, X.; Tang, L.; Fang, Z.; Zheng, Z. Experimental Investigation of Heat Transfer Performance of a Finned-Tube Heat Exchanger under Frosting Conditions. *Sustain. Cities Soc.* **2022**, *80*, 103752. [CrossRef]
25. Che, M.; Elbel, S. Experimental quantification of air-side row-by-row heat transfer coefficients on fin-and-tube heat exchangers. *Int. J. Refrig.* **2021**, *131*, 657–665. [CrossRef]

26. Matos, R.S.; Vargas, J.V.C.; Rossetim, M.A.; Pereira, M.V.A.; Pitz, D.B.; Ordonez, J.C. Performance comparison of tube and plate-fin circular and elliptic heat exchangers for HVAC-R systems. *Appl. Therm. Eng.* **2021**, *184*, 116288. [CrossRef]
27. Sim, J.; Lee, H.; Jeong, J.H. Optimal design of variable-path heat exchanger for energy efficiency improvement of air-source heat pump system. *Appl. Energy* **2021**, *290*, 116741. [CrossRef]
28. Wang, F.; Zhao, R.; Ma, C.; Huang, D.; Qu, Z. Reversely-variable circuitry for finned-tube heat exchanger in air source heat pump to enhance its overall energy performance. *Int. J. Refrig.* **2022**, *142*, 48–57. [CrossRef]
29. Kays, W.M.; London, A.L. *Compact Heat Exchangers*, 3rd ed.; McGraw-Hill: New York, NY, USA, 1984.
30. Browne, M.W.; Bansal, P.K. An elemental NTU-e model for vapour-compression liquid chillers. *Int. J. Refrig.* **2001**, *24*, 612–627. [CrossRef]
31. Browne, M.W.; Bansal, P.K. Challenges in modeling vapor–compression liquid chillers. *ASHRAE Trans.* **1998**, *104*, 474–486.
32. Corberan, J.M.; Fernandez de Cordoba, P.; Ortuno, S.; Ferri, V.; Setaro, T.; Boccardi, G. Modelling of tube and fin coils working as evaporator or condenser. In Proceedings of the 3rd European Thermal Sciences Conference, Heidelberg, Germany, 10–13 September 2000.
33. Corberán, J.M.; García, M. Modelling of plate finned tube evaporators and condensers working with R134a. *Int. J. Refrig.* **1998**, *21*, 273–284. [CrossRef]
34. Jiang, H.; Aute, V.; Radermacher, R. CoilDesigner: A general-purpose simulation and design tool for air-to-refrigerant heat exchangers. *Int. J. Refrig.* **2006**, *29*, 601–610. [CrossRef]
35. McQuiston, F. Heat, mass and momentum transfer data for five plate-fin-tube heat transfer surfaces. *ASHRAE Trans.* **1978**, *84*, 266–293.
36. Tarrad, A.H.; Al-Nadawi, A.K. Modelling of finned-tube using pure and zeotropic blend refrigerants. In Proceedings of the ATINER'S Conference, Athens, Greece, 17–20 December 2015.
37. Joppolo, C.M.; Molinaroli, L.; Pasini, A. Numerical analysis of the influence of circuit arrangement on a fin-and-tube condenser performance. *Case Stud. Therm. Eng.* **2015**, *6*, 136–146. [CrossRef]
38. Tong, L.; Li, H.; Wang, L.; Sun, X.; Xie, Y. The effect of evaporator operating parameters on the flow patterns inside horizontal pipes. *J. Therm. Sci.* **2011**, *20*, 324–331. [CrossRef]
39. Domanski, P.A. Finned-tube evaporator model with a visual interface. In Proceedings of the International Congress of Refrigeration 20th. IIR/IIF, Sydney, Australia, 19–24 September 1999.
40. Domanski, P.A. Simulation of an evaporator with non-uniform one-dimensional air distribution. *ASHRAE Trans.* **1991**, *97*, 793–802.
41. Bensafi, A.; Borg, S.; Parent, D. CYRANO: A computational model for the detailed design of plate-fin-and-tube heat exchangers using pure and mixed refrigerants. *Int. J. Refrig.* **1997**, *20*, 218–228. [CrossRef]
42. Liang, S.Y.; Wong, T.N.; Nathan, G.K. Numerical and experimental studies of refrigerant circuitry of evaporator coils. *Int. J. Refrig.* **2001**, *24*, 823–833. [CrossRef]
43. Ding, X.; Cai, W.; Jia, L.; Wen, C. Evaporator modeling-A hybrid approach. *Appl. Energy* **2009**, *86*, 81–88. [CrossRef]
44. Singh, V.; Aute, V.; Radermacher, R. Numerical approach for modeling air-to-refrigerant fin-and-tube heat exchanger with tube-to-tube heat transfer. *Int. J. Refrig.* **2008**, *31*, 1414–1425. [CrossRef]
45. Oliet, C.; Perez-Segarra, C.D.; Danov, S.; Oliva, A. Numerical simulation of dehumidifying fin-and-tube heat exchangers: Modeling strategies and experimental comparisons. In Proceedings of the International Refrigeration and Air Conditioning Conference, West Lafayette, IN, USA, 16–19 July 2002.
46. Liu, J.; Wei, W.; Ding, G.; Zhang, C.; Fukaya, M.; Wang, K.; Inagaki, T. A general steady state mathematical model for fin-and-tube heat exchanger based on graph theory. *Int. J. Refrig.* **2004**, *27*, 965–973. [CrossRef]
47. Niederer, D.H. Frosting and defrosting effects on coil heat transfer. *ASHRAE Trans.* **1986**, *92*, 467–473.
48. Kondepudi, S.N.; O'Neal, D.L. The effects of frost growth on extended surface heat exchanger performance: A review. *ASHRAE Trans.* **1987**, *93*, 258–277.
49. Kondepudi, S.N.; O'Neal, D.L. Effect of frost growth on the performance of louvered finned tube heat exchangers. *Int. J. Refrig.* **1989**, *12*, 151–158. [CrossRef]
50. Kondepudi, S.N.; O'Neal, D.L. The effects of different fin configurations on the performance of finned-tube heat exchangers under frosting conditions. *ASHRAE Trans.* **1990**, *96*, 439–444.
51. Seker, D.; Karatas, H.; Egrican, N. Frost formation on fin- and- tube heat exchangers. Part II—Experimental investigation of frost formation on fin- and- tube heat exchangers. *Int. J. Refrig.* **2004**, *27*, 375–377. [CrossRef]
52. Kim, K.; Kim, D.R.; Lee, K.-S. Local frosting behavior of a plated-fin and tube heat exchanger according to the refrigerant flow direction and surface treatment. *Int. J. Heat Mass Transf.* **2013**, *64*, 751–758. [CrossRef]
53. Yan, W.-M.; Li, H.-Y.; Wu, Y.-J.; Lin, J.-Y.; Chang, W.-R. Performance of finned tube heat exchangers operating under frosting conditions. *Int. J. Heat Mass Transf.* **2003**, *46*, 871–877. [CrossRef]
54. Zhang, L.; Jiang, Y.; Dong, J.; Yao, Y.; Deng, S. An experimental study on the effects of frosting conditions on frost distribution and growth on finned tube heat exchangers. *Int. J. Heat Mass Transf.* **2019**, *128*, 748–761. [CrossRef]
55. Reichl, C.; Sandström, C.; Hochwallner, F.; Linhardt, F.; Popovac, M.; Emhofer, J. Frosting in heat pump evaporators part A: Experimental investigation. *Appl. Therm. Eng.* **2021**, *199*, 117487. [CrossRef]

56. Lee, K.S.; Kim, W.S.; Lee, T.H. A one dimensional model for frost formation on a cold flat surface. *Int. J. Heat Mass Transf.* **1997**, *40*, 4359–4365. [CrossRef]
57. Tso, C.P.; Cheng, Y.C.; Lai, A.C.K. Dynamic behavior of a direct expansion evaporator under frosting condition, part I. Distributed model. *Int. J. Refrig.* **2006**, *29*, 611–623. [CrossRef]
58. Tso, C.P.; Cheng, Y.C.; Lai, A.C.K. An improved model for predicting performance of finned tube heat exchanger under frosting conditions, with frost thickness variation along fin. *Appl. Therm. Eng.* **2006**, *26*, 111–120. [CrossRef]
59. Yang, D.K.; Lee, K.S.; Song, S. Modeling for predicting frosting behavior of a fin tube heat exchanger. *Int. J. Heat Mass Transf.* **2006**, *49*, 1478–1479. [CrossRef]
60. Padhmanabhan, S.K.; Fisher, D.; Cremaschi, L.; Moallem, E. Modeling non uniform frost growth on a fin and tube heat exchanger. *Int. J. Refrig.* **2011**, *34*, 2018–2030. [CrossRef]
61. Ye, H.Y.; Lee, K.S. Performance prediction of a fin and tube heat exchanger considering air flow reduction due to the frost accumulation. *Int. J. Heat Mass Transf.* **2013**, *67*, 225–233. [CrossRef]
62. Silva, D.L.; Hermes, C.J.L.; Melo, C. First principles modelling of frost accumulation on fan supplied tube fin evaporators. *Appl. Therm. Eng.* **2011**, *31*, 2616–2621. [CrossRef]
63. Chen, H.; Thomas, L.; Besant, R.W. Fan supplied heat exchanger fin performance under frosting conditions. *Int. J. Refrig.* **2003**, *26*, 140–149. [CrossRef]
64. Hwang, J.; Cho, K. Numerical prediction of frost properties and performance of fin-tube heat exchanger with plain fin under frosting. *Int. J. Refrig.* **2014**, *46*, 59–68. [CrossRef]
65. Bhuiyan, A.A.; Islam, A.S. CFD analysis of different fin-and-tube heat exchangers. *J. Mech. Eng.* **2011**, *62*, 237–249.
66. Wang, C.C.; Chang, Y.J.; Hsieh, Y.C.; Lin, Y.T. Sensible heat and friction characteristics of plate fin-and-tube heat exchangers having plane fins. *Int. J. Refrig.* **1996**, *19*, 223–230. [CrossRef]
67. Wang, C.C.; Fu, W.L.; Chang, C.T. Heat transfer and friction characteristics of typical wavy fin-and-tube heat exchangers. *Exp. Therm. Fluid Sci.* **1997**, *14*, 174–186. [CrossRef]
68. Lee, Y.T.; Chien, L.H.; He, J.; Wen, C.-Y.; Yang, A.S. Air side performance characterization of wavy Fin-and-tube heat exchangers having elliptic tubes with large waffle heights. *Appl. Therm. Eng.* **2022**, *217*, 119220. [CrossRef]
69. Rauber, W.K.; Silva, U.F.; Vaz, M.; Alves, M.V.C.; Zdanski, P.S.B. Investigation of the effects of fin perforations on the thermal-hydraulic performance of Plate-Finned heat exchangers. *Int. J. Heat Mass Transf.* **2022**, *187*, 122561. [CrossRef]
70. Li, Y.; Qian, Z.; Wang, Q. Numerical investigation of thermohydraulic performance on wake region in finned tube heat exchanger with section-streamlined tube. *Case Stud. Therm. Eng.* **2022**, *33*, 101898. [CrossRef]
71. Lindqvist, K.; Skaugen, G.; Meyer, O.H.H. Plate fin-and-tube heat exchanger computational fluid dynamics model. *Appl. Therm. Eng.* **2021**, *189*, 116669. [CrossRef]
72. Taler, D.; Taler, J.; Trojan, M. Thermal calculations of plate–fin–and-tube heat exchangers with different heat transfer coefficients on each tube row. *Energy* **2020**, *203*, 117806. [CrossRef]
73. Taler, D.; Taler, J.; Wrona, K. Transient response of a plate-fin-and-tube heat exchanger considering different heat transfer coefficients in individual tube rows. *Energy* **2020**, *195*, 117023. [CrossRef]
74. Zhao, B.; Bi, H.; Wang, H.; Zhou, Y. Experimental and numerical investigation on frosting of finned-tube heat exchanger considering droplet impingement. *Appl. Therm. Eng.* **2022**, *216*, 119134. [CrossRef]
75. Popovac, M.; Emhofer, J.; Reichl, C.H. Frosting in a heat pump evaporator part B: Numerical analysis. *Appl. Therm. Eng.* **2021**, *199*, 117488. [CrossRef]
76. Zdravitsch, F.; Fletcher, C.; Behnia, M. Laminar and turbulent heat transfer predictions in tube banks in cross flow. In Proceedings of the International Conference on Fluid and Thermal Energy Conversion, Denpasar, Indonesia, 12–15 December 1994.
77. Romero-Méndez, R.; Sen, M.; Yang, K.; McClain, R. Effect of fin spacing on convection in a plate fin and tube heat exchanger. *Int. J. Heat Mass Transf.* **2000**, *43*, 39–51. [CrossRef]
78. Tutar, M.; Akkoca, A.; Oztekin, S.; Turkey, B.A. A numerical study of heat transfer and fluid flow in a plate fin-and-tube heat exchanger. *Asme-Publications-Pvp* **2001**, *431*, 77–84.
79. Zhang, W.J.; Zhang, C.L. A generalized moving-boundary model for transient simulation of dry-expansion evaporators under larger disturbances. *Int. J. Refrig.* **2006**, *29*, 1119–1127. [CrossRef]
80. Willatzen, M.; Pettit, N.B.O.L.; Ploug-Sørensen, L. A general dynamic simulation model for evaporators and condensers in refrigeration. Part I: Moving-boundary formulation of two-phase flows with heat exchange. *Int. J. Refrig.* **1998**, *21*, 398–403. [CrossRef]
81. Pettit, N.B.O.L.; Willatzen, M.; Ploug-Sørensen, L. A general dynamic simulation model for evaporators and condensers in refrigeration. Part II: Simulation and control of an evaporator. *Int. J. Refrig.* **1998**, *21*, 404–414. [CrossRef]
82. Shao, L.L.; Zhang, C.L. Logic unconstrained multi-zone evaporator and condenser models. *Int. J. Refrig.* **2007**, *30*, 926–931. [CrossRef]
83. Illán-Gómez, F.; García-Cascales, J.R.; Molina-Valverde, R.; Velasco, F.J.S. A discretization method for the characterization of a plate heat exchanger working as evaporator during transient conditions. *Int. J. Therm. Sci.* **2023**, *184*, 107998. [CrossRef]
84. Starace, G.; Fiorentino, M.; Longo, M.P.; Carluccio, E. A hybrid method for the cross flow compact heat exchangers design. *Appl. Therm. Eng.* **2017**, *111*, 1129–1142. [CrossRef]

85. Carluccio, E.; Starace, G.; Ficarella, A.; Laforgia, D. Numerical analysis of a cross-flow compact heat exchanger for vehicle applications. *Appl. Therm. Eng.* **2005**, *25*, 1995–2013. [CrossRef]
86. Fiorentino, M.; Starace, G. The design of countercurrent evaporative condensers with the hybrid method. *Appl. Therm. Eng.* **2018**, *130*, 889–898. [CrossRef]
87. Starace, G.; Fiorentino, M.; Meleleo, B.; Risolo, C. The hybrid method applied to the plate-finned tube evaporator geometry. *Int. J. Refrig.* **2018**, *88*, 67–77. [CrossRef]
88. Starace, G.; Macchitella, S.; Fiorentino, M.; Colangelo, G. Influence of circuit arrangement on evaporator performance using the hybrid method. In Proceedings of the 6th IIR Conference on Thermophysical Properties and Transfer Processes of Refrigerants, Vicenza, Italy, 1–3 September 2021.
89. Starace, G.; Macchitella, S.; Colangelo, G. The hybrid method for the plate-finned tube evaporator design process. In Proceedings of the 76° ATI Conference, Rome, Italy, 15–17 September 2021.
90. Starace, G.; Macchitella, S.; Colangelo, G. Improvements to the hybrid method applied to the design of plate-finned tube evaporators. In Proceedings of the 77° ATI Conference, Bari, Italy, 12–14 September 2022.
91. Yun, J.Y.; Lee, K.S. Influence of design parameters on the heat transfer and flow friction characteristics of the heat exchanger with slit fins. *Int. J. Heat Mass Transf.* **2000**, *43*, 2529–2539. [CrossRef]
92. Matos, R.S.; Laursen, T.A.; Vargas, J.V.C.; Bejan, A. Three-dimensional optimization of staggered finned circular and elliptic tubes in forced convection. *Int. J. Therm. Sci.* **2004**, *43*, 477–487. [CrossRef]
93. Wang, C.-C.; Jang, J.-Y.; Lai, C.-C.; Chang, Y.-J. Effect of circuit arrangement on the performance of air-cooled condensers. *Int. J. Refrig.* **1999**, *22*, 275–282. [CrossRef]
94. Ding, W.K.; Fan, J.F.; He, Y.L.; Tao, W.Q.; Zheng, Y.X.; Gao, Y.F.; Song, J. A general simulation model for performance prediction of plate fin-and-tube heat exchanger with complex circuit configuration. *Appl. Therm. Eng.* **2011**, *31*, 3106–3116. [CrossRef]
95. Saleem, S.; Bradshaw, C.R.; Bach, C.K. Validation of a multi-circuit heat exchanger model for evaluating the effect of refrigerant circuitry on cross-fin conduction in evaporator mode. *Int. J. Refrig.* **2021**, *131*, 623–633. [CrossRef]
96. Bach, C.K.; Groll, E.A.; Braun, J.E.; Horton, W.T. Mitigation of air flow maldistribution in evaporators. *Appl. Therm. Eng.* **2014**, *73*, 879–887. [CrossRef]
97. Cen, J.; Hu, J.; Jiang, F. An automatic refrigerant circuit generation method for finned-tube heat exchangers. *Can. J. Chem. Eng.* **2018**, *96*, 2661–2672. [CrossRef]
98. Domanski, P.A.; Yashar, D. Optimization of finned-tube condensers using an intelligent system. *Int. J. Refrig.* **2007**, *30*, 482–488. [CrossRef]
99. Domanski, P.A.; Yashar, D.; Kaufman, K.A.; Michalski, R.S. An optimized design of finned-tube evaporators using the learnable evolution model. *HVACR Res.* **2004**, *10*, 201–211. [CrossRef]
100. Yashar, D.; Wojtusiak, J.; Kaufman, K.; Domanski, P.A. A dual-mode evolutionary algorithm for designing optimized refrigerant circuitries for finned-tube heat exchangers. *HVACR Res.* **2012**, *18*, 834–844.
101. Wu, Z.; Ding, G.; Wang, K.; Fukaya, M. Application of a genetic algorithm to optimize the refrigerant circuit of fin-and-tube heat exchangers for maximum heat transfer or shortest tube. *Int. J. Therm. Sci.* **2008**, *47*, 985–997. [CrossRef]
102. Wu, Z.; Ding, G.; Wang, K.; Fukaya, M. Knowledge-based evolution method for optimizing refrigerant circuitry of fin-and tube heat exchangers. *HVACR Res.* **2008**, *14*, 435–452. [CrossRef]
103. Ye, H.-Y.; Lee, K.-S. Refrigerant circuitry design of fin-and-tube condenser based on entropy generation minimization. *Int. J. Refrig.* **2012**, *35*, 1430–1438. [CrossRef]
104. Lee, W.-J.; Kim, H.J.; Jeong, J.H. Method for determining the optimum number of circuits for a fin-tube condenser in a heat pump. *Int. J. Heat Mass Transf.* **2016**, *98*, 462–471. [CrossRef]
105. Goldberg, D.E. *Genetic Algorithms in Search, Optimization and Machine Learning*; Addison-Wesley: Boston, MA, USA, 1989.
106. Li, Z.; Aute, V.; Ling, J. Tube-fin heat exchanger circuitry optimization using integer permutation based Genetic Algorithm. *Int. J. Refrig.* **2019**, *103*, 135–144. [CrossRef]
107. Gholap, A.K.; Khan, J.A. Design and multi-objective optimization of heat exchangers for refrigerators. *Appl. Energy* **2007**, *84*, 1226–1239. [CrossRef]
108. Ploskas, N.; Laughman, C.; Raghunathan, A.U.; Sahinidis, N.V. Optimization of circuitry arrangements for heat exchangers using derivative-free optimization. *Chem. Eng. Res. Des.* **2017**, *131*, 16–28. [CrossRef]
109. Ishaque, S.; Kim, M.-H. Refrigerant circuitry optimization of finned tube heat exchangers using a dual-mode intelligent search algorithm. *Appl. Therm. Eng.* **2022**, *212*, 118576. [CrossRef]
110. Dehaj, M.S.; Hajabdollahi, H. Fin and tube heat exchanger: Constructal thermo-economic optimization. *Int. J. Heat Mass Transf.* **2021**, *173*, 121257. [CrossRef]
111. Xie, C.; Yan, G.; Ma, Q.; Elmasry, Y.; Singh, P.K.; Algelany, A.M.; Wae-hayee, M. Flow and heat transfer optimization of a fin-tube heat exchanger with vortex generators using Response Surface Methodology and Artificial Neural Network. *Case Stud. Therm. Eng.* **2022**, *39*, 102445. [CrossRef]